AD-A044 734 CORNELL UNIV ITHACA N Y MATERIALS SCIENCE CENTER F/G 20/3
FUNDAMENTAL FLUXOID-DEFECT INTERACTIONS IN IRRADIATED SUPERCOND--ETC(U)
JUN 77 E J KRAMER AFOSR-77-3107
UNCLASSIFIED MSC-2857 AFOSR-TR-77-1189 NL

1 OF 1
ADA044734

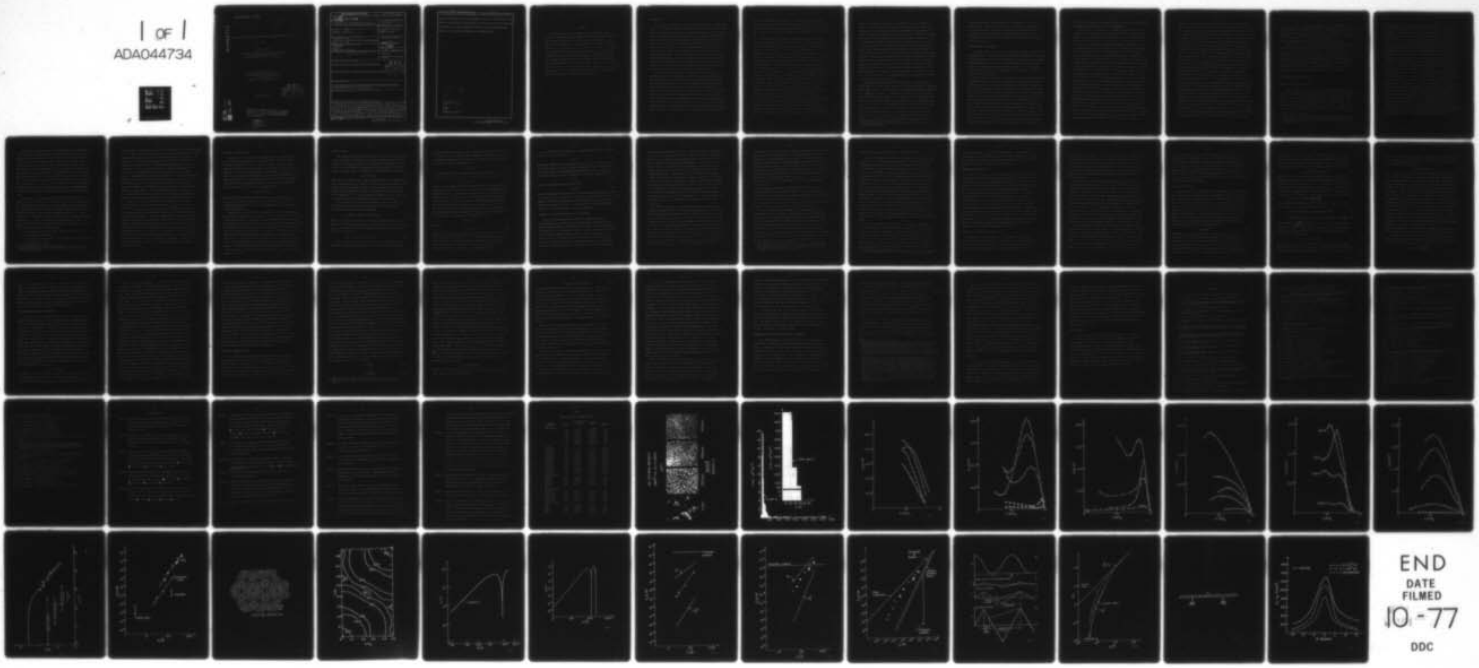

END
DATE FILMED
10-77
DDC

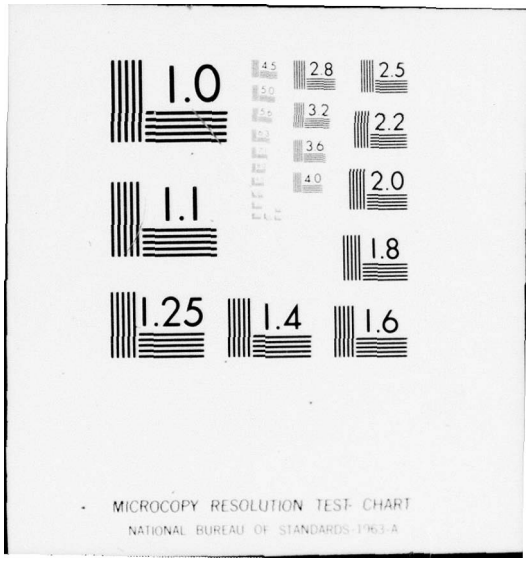
1.0
1.1
1.25
1.4
1.6
1.8
2.0
2.2
2.5
2.8
3.2
3.6
4.0
4.5
5.0
5.6
MICROCOPY RESOLUTION TEST CHART
NATIONAL BUREAU OF STANDARDS-1963-A

FUNDAMENTAL FLUXOID-DEFECT INTERACTIONS IN IRRADIATED SUPERCONDUCTORS

by

Edward J. Kramer

Department of Materials Science and Engineering
and the Materials Science Center
Cornell University, Ithaca, New York 14853

presented at the
International Discussion Meeting on
Radiation Effects on Superconductivity
13-16 June 1977

Submitted to J. Nuclear Materials

MSC Report #2857

SECURITY CLASSIFICATION OF THIS PAGE (When Data Entered)

REPORT DOCUMENTATION PAGE

READ INSTRUCTIONS BEFORE COMPLETING FORM

1. REPORT NUMBER: AFOSR-TR-77-1189
2. GOVT ACCESSION NO.
3. RECIPIENT'S CATALOG NUMBER

4. TITLE (and Subtitle): FUNDAMENTAL FLUXOID-DEFECT INTERACTIONS IN IRRADIATED SUPERCONDUCTORS
5. TYPE OF REPORT & PERIOD COVERED: INTERIM rept.
6. PERFORMING ORG. REPORT NUMBER

7. AUTHOR(s): Kramer, Edward J.
8. CONTRACT OR GRANT NUMBER(s): AFOSR-77-3107

9. PERFORMING ORGANIZATION NAME AND ADDRESS
Cornell University
Department of Materials Science and Engineering
Ithaca, NY 14853
10. PROGRAM ELEMENT, PROJECT, TASK AREA & WORK UNIT NUMBERS: 61102F-2306-C1

11. CONTROLLING OFFICE NAME AND ADDRESS
AFOSR/NE
Bldg 410
Bolling AFB, DC 20332
12. REPORT DATE: June 1977
13. NUMBER OF PAGES: 63

14. MONITORING AGENCY NAME & ADDRESS (if different from Controlling Office)
15. SECURITY CLASS. (of this report): UNCLAS
15a. DECLASSIFICATION DOWNGRADING SCHEDULE

16. DISTRIBUTION STATEMENT (of this Report)

Approved for public release; distribution unlimited.

17. DISTRIBUTION STATEMENT (of the abstract entered in Block 20, if different from Report)

18. SUPPLEMENTARY NOTES

INTERNATIONAL DISCUSSION MEETING ON RADIATION EFFECTS ON SUPERCONDUCTIVITY, 13-16 June 1977.

19. KEY WORDS (Continue on reverse side if necessary and identify by block number)

20. ABSTRACT (Continue on reverse side if necessary and identify by block number)

Flux pinning experiments in irradiated superconductors which make it possible to independently vary the defect density ρ and elementary interaction force f_p between the defect and the fluxoid lattice are reviewed. A new measure of flux pinning, Q, the volume pinning force per defect, is introduced and is shown to be independent of ρ for $\rho < 10^{22}$ m^{-3}. In Nb at B=.5 B_{c_2} and 4.2K, $Q = 5\times10^{-18}$N for Frenkel defects, 3×10^{-16}N for cascades, 2×10^{-15}N for 100 Å dislocation loops and 3×10^{-14}N for 100Å voids. The Q's for voids and loops increase

DD FORM 1 JAN 73 1473 EDITION OF 1 NOV 65 IS OBSOLETE

UNCLASSIFIED 400143

SECURITY CLASSIFICATION OF THIS PAGE (When Data Entered)

20. strongly with void or loop diameter. Accurate estimates of f_p for voids and dislocation loops can be made and plotted versus Q. The results for the two defects overlap forming a single master curve that can be used as an experimental solution to the summation problem. Reasons why current summation models do not reproduce the master curve are discussed.

ABSTRACT

Flux pinning experiments in irradiated superconductors which make it possible to independently vary the defect density ρ and elementary interaction force f_p between the defect and the fluxoid lattice are reviewed. A new measure of flux pinning, Q, the volume pinning force per defect, is introduced and is shown to be independent of ρ for $\rho < 10^{22} m^{-3}$. In Nb at $B = .5\ Bc_2$ and 4.2K, $Q = 5 \times 10^{-18} N$ for Frenkel defects, $3 \times 10^{-16} N$ for cascades, $2 \times 10^{-15} N$ for 100Å dislocation loops and $3 \times 10^{-14} N$ for 100Å voids. The Q's for voids and loops increase strongly with void or loop diameter. Accurate estimates of f_p for voids and dislocation loops can be made and plotted versus Q. The results for the two defects overlap forming a single master curve that can be used as an experimental solution to the summation problem. Reasons why current summation models do not reproduce the master curve are discussed.

INTRODUCTION

The critical current density J_c in type II superconductors is extraordinarily sensitive to the defect structure of the material. The reason for this sensitivity has been qualitatively understood for at least twelve years[1-4]. At high magnetic fields the field penetrates the superconductor in the form of a lattice of singly quantized current vortices (flux quantum $\phi_o = 2 \times 10^{-7}$ gauss cm^2). When a transport current is applied to the superconductor a Lorentz force acts on the vortex or fluxoid lattice (FLL) and in perfectly homogeneous materials, this force would cause the FLL to move and dissipate energy viscously, leading to appearance of a voltage across the current leads. The introduction of a defect on the other hand changes the free energy of the FLL in its vicinity. To move the FLL in a superconductor containing crystal defects now requires that a critical value of the Lorentz force $J_c \times B$ be exceeded. This critical value F_p we call the global pinning force per unit volume (or less exactly just the pinning force).

To construct a quantitative theory of F_p we need to first determine the elementary interaction force f_p between a single defect (pinning center) and the FLL and then sum these elementary interactions in a proper statistical manner to find the global pinning force density. This summation problem has proved to be most refractory and it is safe to say that there is no general agreement in the field as to the correct approach. The principal difficulty is how to take account of the rigidity of the FLL. This rigidity logically must prevent all pinning centers from contributing their maximum value of the elementary interaction force f_p to the global average; indeed a perfectly rigid FLL interacting with a randomly distributed array of pinning centers will have a zero global pinning force regardless of the value of f_p of these centers. For any position of the rigid FLL there

will be as many elementary interaction forces acting in the positive as in the negative coordinate direction leading to complete concellation. Only if the FLL is allowed to relax elastically between pinning centers will the F_p be non-zero. The elasticity of the FLL must be expected to play an important role in determining F_p.

One further factor which complicates the problem of comparing calculations of F_p with the measured values of the quantity for technological superconductors, such as NbTi or Nb_3Sn, is that the metallurgical structure of these materials is difficult to define exactly. It is difficult to determine what changes heat treatment causes in the dislocation cell walls in NbTi, for example. Does it cause dislocation rearrangement in and regularization of these walls or does it allow segregation of interstitial impurity atoms to these defects? It is difficult, if not impossible, to independently change the density of pinning centers and their elementary interaction force in these systems even if one knew enough about the microstructure to calculate f_p. For this reason most quantitative comparisons between flux pinning theory and experiment have relied on experiments in model metallurgical systems. These are superconductors, which while not of great technological interest, can be manipulated in such a way to introduce a particular species of defect of known size and concentration. Clearly irradiated elemental superconductors have the potential to be good model systems. In particular by changing the conditions of irradiation one can change the species of defect introduced and/or the average size of the defect. At the same time by controlling the irradiation dose and low level impurity content one can control the defect density. Nevertheless, one must be on guard against the introduction of irradiation-produced defect structures other than those intended. There is no substitute for direct electron microscopic observation of the structure

produced. One example should suffice as an object lesson. My colleagues and I wanted to measure the flux pinning due to dislocation loops produced by neutron irradiation in an alloy system in which we could change the thermodynamic critical field H_c by changing the composition of the alloy. We chose the NbMo system because there were no long lived radioactive decay products produced and because the published Nb-Mo phase diagram shows complete solid solubility so that H_c could be decreased continuously to zero by adding more and more Mo. When we examined irradiated samples in the transmission electron microscope, we found no dislocation loops but rather a quasi-periodic contrast modulation along certain crystallographic directions. With more work we determined that the Nb-Mo system undergoes a spinodal decomposition at low temperatures that is accelerated by the neutron irradiation and that one of the peaks in F_p as a function of magnetic field was due to the "matching" of FLL spacing to the spacing of the composition modulation[5]. Needless to say if we had not looked at the defect structure of our samples, we might still be trying to concoct a flux pinning mechanism that would give us a "matching" peak from an array of dislocation loops.

Although there has been much interest in irradiation of compound and alloy superconductors* for technological reasons, we will confine this paper to irradiation effects on the pinning in "dirty" niobium, i.e., Nb with a Ginzburg-Landau parameter $\kappa_1 (\kappa_1 = \frac{H_{c_2}}{\sqrt{2} H_c})$ which exceeds 1.2. These values of κ are above the upper threshold for type II/I superconductivity[6]. At κ's lower than $\simeq$1.2 the superconductor exhibits a first order phase transition (discontinuous increase in magnetization) at H_{c_1} due to an attractive interaction between vortices. The only samples that may be below this threshold are the ones used for the very low dose electron and neutron low temperature irradiations. The advantage of using niobium for this comparison is that it should be possible to compare the effects of different defects on F_p without having to correct for changes in the properties of the

* These materials will be discussed by A. Sweedler and by S. Sekula in other papers in this conference.

superconducting matrix in which these defects are embedded, since unlike the superconducting compounds there is little or no change in the thermodynamic critical field of Nb with irradiation. In addition the data needed as input for computing f_p is mostly available as are a number of "model" studies of flux pinning by precipitates and dislocations to which one can compare the irradiated superconductor results.

DEFECTS PRODUCED BY IRRADIATION

In niobium different defects can be introduced by irradiating the crystal with different particles. Irradiation by 3 MeV electrons at 4.6°K produces statistically distributed Frenkel defects (vacancy and interstitial atom pairs) which are immobile at these temperatures. The size of a Frenkel pair in Nb (the vacancy and interstitial) can be estimated from the recombination volume to be $\simeq 5$ Å in diameter. A comprehensive investigation of flux pinning by these defects has been made by Ullmaier and his coworkers[7,8].

Neutron irradiation of niobium at 4.6°K, however, results in cascade production. A cascade is thought to consist of a central depleted zone (vacancy rich region) surrounded by a cloud of interstitial atoms that have been ejected from this depleted zone by replacement collision sequences[9,10,11]. The diameter of the interstitial cloud in Nb is uncertain but a rough estimate is $\sim$150Å[12]. The number of vacancies in the depleted zone can be computed to be $220E_n$, where E_n is the incident neutron energy, in MeV, using a modified form[13] of the Kinchin-Pease model[14] with a displacement efficiency of 0.8. The size distribution of depleted zones, and for that matter the interstitial clouds surrounding them, thus depends rather critically on the reactor fast neutron spectrum used to produce the damage. Since reactor spectra are typically rather broad (the CPS reactor at Argonne has significant flux from .2 MeV to 7 MeV for example[12]), one must expect a broad distribution of cascade sizes within a given irradiated specimen. Investigations of

flux pinning in niobium by low temperature neutron irradiation have been published by Berndt, Kartascheff and Wenzl[15] and by Brown[16,12].

Dislocation loops can be produced in niobium by either fast neutron or ion irradiation at room temperature and it is well established that sequential fast neutron doses at room temperature produce increases in flux pinning[17,18,19]. However in the interpretation of the results it is crucial that the dislocation loop structure be observed directly with the transmission electron microscope. Interstitial impurities such as oxygen can act as nucleating centers for aggregation of mobile point defects to form dislocation loops[20] so that changes in the residual impurity content of the niobium from experiment to experiment can lead to changes in the average dislocation loop density and size. Figure 1 shows transmission electron micrographs of niobium specimens doped with different oxygen concentrations which were all irradiated to the same fast neutron dose of 9×10^{19} nvt (neutrons/cm^2). In the specimen with the lowest oxygen doping level large dislocation loops are visible whereas in the other specimens the damage is in the form of "black spots" (unresolved dislocation loops) which decrease in size and increase in density as the oxygen doping level increases. From micrographs like these, histograms representing the dislocation loop density distribution as a function of loop diameter can be constructed. Two such histograms representing the extreme oxygen content are shown in Figure 2. An investigation of the flux pinning in these samples has been carried out by Agrawal, Kramer and Loomis[21]. Recently Rollins and Anjaneyulu[22] have reported measurements of the critical current density as a function of distance from the surface in Nb irradiated by protons at room temperature. While no microscopy was carried out on these samples, the investigators could compute the depth dependence of the size of the dislocation loops produced by assuming that all loops nucleate at impurity atoms and by assuming the point defect production rate at each depth to be given by

Rutherford scattering theory and the Kinchin-Pease[14] model of atomic displacements. Their results for the dependence of F_p on dislocation loop diameter are in basic agreement with those from room temperature neutron irradiation experiments[21].

Finally, it is possible to produce voids in niobium by irradiating with neutrons or ions at high temperatures, $600°C < T < 1000°C$. In general metals will undergo "void swelling" in an intermediate temperature range well below the melting point but well above the temperature at which vacancies are mobile. This phenomenon is thought to be due to slight bias for trapping of interstitials at dislocation loops over trapping of vacancies, due to the stronger elastic interaction of the former, leading to high vacancy supersaturations which result in void nucleation and growth[23]. Two investigations of flux pinning by irradiation-induced voids have been carried out by Freyhardt[24] and by Koch, Freyhardt and Scarborough[25]. In one case voids were produced by 3.5 MeV Ni^+ ion bombardment at temperatures between 780 and 865°C[24]. In the other set of experiments, niobium samples were irradiated in the EBR II facility at temperatures between 650°C and 1080°C to fast neutron (>1 MeV) fluences of $\sim 10^{22}$ nvt (neutrons/cm^2). In each case the void size distribution was directly determined with transmission electron microscopy. The Ni^+ ion irradiation method of introducing voids has many experimental advantages over neutron irradiation. The maximum displacement rate for 3.5 MeV Ni^+ of 5×10^{-3} DPA/sec is approximately 5000 times higher than that for neutron irradiation[24] so ion irradiation times are far shorter. In addition the ion-irradiation samples do not become radioactive and do not require the long "cooling off" period neutron irradiated samples do. Nevertheless the fact that the voids are confined to a layer about 1.5μm below the surface of the foil at a depth near the end of the Ni^+ ion range somewhat complicates the interpretation of the results of these experiments[24]. It appears also that the density of voids is about a

factor of ten higher at comparable temperatures for the ion-irradiated samples as compared with the neutron-irradiated samples. The increased void density may reflect enhanced point defect trapping and void nucleation at the implanted Ni atoms (for 50 DPA there are about 2×10^{26} Ni atoms/m^2 in the irradiated layer) or it may reflect similar enhancement by the higher oxygen atom content in these samples.

Voids produced by these irradiations are usually approximately randomly distributed* but in a narrow temperature range ~800°C±20°C for high oxygen contents a b.c.c. void lattice has been observed[24,26]. Such a regular array of voids would represent an ideal model system with which to test theories of both the elementary interaction force and the summation problems. Freyhardt[24] has reported results on a sample with 100Å voids and a lattice constant of about 380Å. Clearly more experiments on void lattices with different void size and lattice spacings will be necessary before any general conclusions can be drawn.

EXPERIMENTAL FLUX PINNING RESULTS

Magnetic Field Dependence of F_p:

Since the magnetic field dependence of both the elementary interaction force and the elastic constants of the FLL, which govern the response of this lattice to f_p, can be most conveniently expressed as functions of reduced magnetic induction $b = B/B_{c_2}$ it is now conventional to compare the field dependence of F_p of one sample with another by plotting the data as F_p vs b. Figures 3 through 6 show the dependence of F_p on magnetic induction for flux pinning by Frenkel pairs[7],

---

* It is clear that a truly random arrangement of either voids or dislocation loops cannot be achieved since there is a strong tendency for closely spaced defects not to develop since they would drain approximately the same volume of point defects.

by cascades[15], by dislocation loops[21] and by voids[24]. The different curves in each figure represent different defect densities in the case of Frenkel pairs and cascades or combinations of different defect densities and sizes in the case of dislocation loops and voids. The relevant specimen parameters are given in Table I for each curve. Defect densities ρ were taken to be the values determined in [7] from the resistivities of a Frenkel pair and those determined in [15] from the relation between cascade density and neutron fluence, whereas for dislocation loops and voids the densities determined directly by TEM observations of [21] and [24] were used. The $F_p(b)$ curves for the different defects have certain features in common. Most show a maximum of F_p vs b with F_p approaching zero at b = 1. For pinning by Frenkel pairs however F_p increases significantly from zero only below b = .8 to b = .9 with this limit increasing with increasing electron fluence. For the low electron fluence samples also any maximum in F_p is at reduced inductions below b = .4 but as the fluence is increased, a maximum appears and shifts upward in reduced field to b = .55 at the highest fluence. Both the dislocation loop samples and the cascade samples show a peak effect, a narrow peak in the pinning force vs. b just below b = 1 in some of the samples. For cascade pinning a small sharp peak develops just below b = 1 at the lowest fluences, increases in size and shifts to lower b, becoming much broader at the higher cascade densities. At the highest cascade density there is a decrease in F_p on the low b side of the peak and a perceptible narrowing of the peak. However, for the dislocation loops the peak is broad and below b = .85 for low loop densities but shifts to higher reduced inductions and narrows as the loop density increases. Clearly the changes in the peak effect are not only a function of defect density but must also involve the elementary interaction force f_p which will depend on defect size.

The magnetic field dependence of void pinning appears to be somewhat different from either cascade or dislocation loop pinning in that there is a broad maximum in the pinning that occurs at relatively low reduced fields between $b = .7$ and $b = .3$ for all samples. However, there is no unique shape to the F_p vs b curve; different microstructures give different shapes as in the case of the other defect species. Furthermore the F_p vs b curves are more sensitive to microstructure at low b than at high b. For example the ratio of F_p for two different void microstructures is at least a factor of two larger at $b = .5$ than at $b = .9$. This enhanced structure sensitivity of the pinning force at low b is even more strikingly evident in the F_p vs. b curves (Figure 7) for the void structures produced by neutron irradiation where the curves practically superimpose above $b = .9$[25]*. This behavior is very similar to that of the samples with the peak effect.

The peak effect is thought to arise due to the softening of the FLL at inductions just below B_{c_2}[27]. Two possibilities exist for the mechanism limiting F_p on the high b side of the peak. In the first proposed Campbell and Evetts[2] full "synchronization" of pins occurs at the peak and further softening of the flux lattice at higher b does not result in further increases in F_p. In the second[28] it is supposed that the FLL can plastically shear around the strongest pins leading to a F_p that is insensitive to f_p and only moderately sensitive to pin density. These models are discussed in more detail elsewhere[29,4]. Present evidence that seems to favor the latter model is:

1) The disappearance of flux line lattice history effects on F_p at b's greater than the peak[30,31,32]

2) An abrupt change in the character of the voltage-current characteristic[33] at b's just above the peak.

---

* Errors in determining H_{c_2}, which are especially hard to avoid when H_{c_2} is measured resistively due to surface superconductivity, will shift the H_{c_2} curves in Figure 6 significantly.

Recent theoretical developments have combined to eliminate some of the objections to the FLL shear model. In the original model it was necessary that line pinning occur[28]. Schmucker[34] has shown point pins can initiate FLL shear and that depending on the aspect ratio of the pins any b dependence of F_p between (1-b) and $(1-b)^2$ can be obtained in the region near B_{c_2}. In Schmucker's model unfortunately there is no possibility of a crossover from pin breaking to a FLL shear mechanism as b increases since both mechanisms have the same b dependence in the point pinning limit. Brandt[35-39] has recently shown however that for short wavelength deformations both C_{44}, the tilt modulus, and C_{11}, the compression modulus, of the FLL become very small at H_{c_2}. [It had been previously accepted following the zero wave vector calculation of Labusch[40] that C_{11} and C_{44} increased as B^2 and were much larger than C_{66} near B_{c_2}. The shear modulus C_{66} decreases as $(1-b)^2$ near B_{c_2}, a result Brandt extends to all wave vectors.] Schmucker and Brandt[41] have shown that the displacement produced by a point pin increases drastically above $b \simeq .8$ whereas with the Labusch approximation this displacement is constant. Since FLL shear at a point pin involves creation of a flux line lattice dislocation (FLD) loop whose line tension is proportional to $\sqrt{C_{11}C_{44}}$ and since only short range displacements are produced by a small loop one expects that the force to create a FLD loop above $b \simeq .8$ will be significantly less than that originally computed by Schmucker[34] who used Labusch's expression for C_{44}. The theoretical situation regarding the peak effect and the interpretation of the high field F_p is thus far from settled at the moment, but many new ideas have surfaced which are currently being explored. In any case with the exception of the very weakly pinning electron irradiated Nb, irradiated niobium samples appear to behave near B_{c_2} very much like Nb and its alloys containing other defects[42]. In what follows our discussion will center primarily on the structure sensitive F_p at magnetic inductions well below B_{c_2}.

Temperature Dependence of F_p:

Pinning force vs. b curves have been measured at various temperatures only for void structures produced by Ni^+ ion irradiation[24]. Figure 8 shows the temperature dependence of the F_p vs b curve of one sample in Figure 6. While changes in temperature produce large changes in the magnitude of the peak in F_p they leave its shape essentially unchanged. Indeed if $F_p/F_{p_{max}}$ where $F_{p_{max}}$ is the value of F_p at the peak is plotted against b all these curves superimpose into a single master curve. This scaling behavior first discovered by Fietz and Webb[43] is exhibited by most hard superconductors[28]. A suitable scaling parameter is B_{c_2} so that one has the phenomenological expression for F_p:

$$F_p = (B_{c_2}(T))^m \, g(b) \qquad (1)$$

where g(b) is only a function of reduced field and can be evaluated from any F_p vs b curve at constant temperature, such as those in Figs. 3-7. For void pinning Freyhardt[24] finds that $m \simeq 4$ at low temperature but that m increases to ~ 2 at temperatures near T_c.

Although scaling has been found to fail badly for a number of superconductors, usually this can be attributed to: (1) samples that have a paramagnetically limited B_{c_2} at low temperatures[44], (2) inhomogeneous samples in which a minor but continuous superconducting path exists with a higher T_c than the majority of the sample[45,46,47], (3) samples with a sufficiently regular defect microstructure that a peak in the pinning force develops due to a matching of a FLL spacing to the spacing of defects[48-55]. Since the irradiated samples described are homogeneous, are non-paramagnetically limited and have a random defect structure (with the exception of the void lattice), it is a reasonable assumption that the scaling law will hold approximately for these materials. Nevertheless experiments on the temperature dependence of flux pinning in samples with well characterized dislocation loops as well as samples with cascades should be carried out.

Summation Models:

Before beginning our discussion of the effects of pin density on flux pinning, it will be useful to review briefly the two models currently used most often as solutions to the summation problem. One model proposed by Dew-Hughes[58] is that the FLL in hard superconductors is amorphous and flexible enough to optimally contact all pinning centers in the material. He then obtains the direct summation

$$F_p = \sum_i \rho(i) f_p(i) \tag{2}$$

where $\rho(i)$ is the number density of the ith species of defect with maximum elementary interaction force $f_p(i)$. Whatever one's view of the radical assumptions necessary for this direct summation to hold, it has one undeniably useful feature that has not been emphasized in the past. It predicts an absolute upper limit for the pinning force. It is not possible for any summation model to result in an F_p greater than sum of the maximum interaction force of all the defects.

The point pinning model developed by Labusch[57] is much more widely used currently because it explicitly takes the rigidity of the FLL into account. In the form this model is usually cast F_p becomes

$$F_p = \left(\frac{d}{a_o}2\right) \sum_i \rho(i) f_p(i) \cdot [f_p(i)/4\pi a_o \mu_{eff}] \tag{3}$$

where a_o is the flux line spacing, d is the half the interaction width of the pinning center which approximately equals the coherence length ξ for small defects, and μ_{eff} is an effective modulus for deformation of the FLL by a point force normal to the flux lines[40].

$$\mu_{eff} = \pi^{-1/2}[(C_{44}C_{66})^{-1/2} + (C_{44}C_{11})^{-1/2}]^{-1} \tag{4}$$

In Eq. 3 the term in brackets in the sum is equal to the displacement u of the FLL by the maximum interaction force f_p. The ratio u/a_o can be considered

an efficiency factor with which to correct the direct summation for the effects of FLL rigidity. Since an arbitrary FLL displacement u produced by a defect implies an elementary interaction force $f = (4\pi a_o \mu_{eff})\, u = ku$ the FLL responds as an elastic spring with spring constant k equal to

$$k = 4\pi a_o \mu_{eff} \tag{5}$$

An important restriction in Labusch's theory that is often ignored in practice is that f_p satisfy the threshold criterion, which can be written as [21].

$$f_p >> 2\mu_{eff} a_o^2 \tag{6}$$

If f_p is less than threshold the Labusch theory predicts $F_p = 0$ and unless the elementary pinning force is well above threshold F_p is significantly smaller than that predicted by Eq. 3. An expression similar to Eq. 3 can be derived from the dynamic hysteresis of FLL motion past pins[58-60] and exactly the same threshold criterion applies. There is also an important and dubious assumption regarding the nature of the energy well giving rise to the elementary interaction force of the defect hidden in both the statistical and dynamic theories of pinning; we will consider this assumption in detail after comparing theory with experiment.

To facilitate this comparison let us rewrite Eq. 3 as

$$F_p = \rho C f_p^2 \tag{7}$$

and Eq. 2 as

$$F_p = \rho f_p \tag{8}$$

where $C = \xi/(4\pi a_o^3 \mu_{eff})$, $f_p^2 = \Sigma\rho(i) f_p^2(i)/\rho$ and $f_p = \Sigma\rho(i) f_p(i)/\rho$. We will subsequently ignore the fact that $\langle f_p^2 \rangle^{1/2} \neq \langle f_p \rangle$ on the grounds that the errors produced in doing so are relatively small[24,21]. When actually comparing f_p for microstructure consisting of a range of defect sizes and thus f_p's, we will actually use $\langle f_p^2 \rangle^{1/2}$ as the appropriate f_p for comparison purposes.

Let us now introduce a new quantity, the specific pinning force Q, or the pinning force per defect defined as

$$Q \equiv F_p/\rho \tag{9}$$

which can be computed from the experimental F_p and ρ values. If either of the two summation models is correct Q should be independent of defect density and thus be a direct measure of the maximum elementary interaction force of a single defect and the response of the FLL to that force. If the direct summation holds

$$Q = f_p \tag{10}$$

whereas if the Labusch statistical theory holds

$$Q = Cf_p^2 \tag{11}$$

Even if neither summation model holds, if we can experimentally establish that the specific pinning force is approximately independent of pin density we can use Q as a relative measure of the pinning effectiveness of different defect species under conditions where the FLL rigidity is the same. In the next section we will show experimentally that if ρ is not too large, Q is in fact independent of ρ.

Dependence of the Specific Pinning Force on Pin Density:

Since the specific pinning force density will be sensitive through its strong dependence on f_p to the size of the pinning defect (defect size is one of the most important factors in determining f_p[4]), the best test of the pin density independence of Q is to introduce more and more defects of constant size and determine experimentally whether Q remains constant. Here low temperature radiation damage experiments are unexcelled since by increasing the neutron or electron fluence we can increase the cascade or Frenkel pair density without changing the defect size distribution, which is a function only of the reactor neutron energy

spectrum or the electron energy. Of course to fairly compare Q's if the statistical theory is correct we must make sure that the FLL compliance, represented by C in Eq. 7, is held constant, and this requirement poses a problem since B_{c_2} and κ increase during the low temperature irradiations due to the increase in resistivity. However it turns out that the FLL compliance at constant b is approximately constant over the range of κ from 1.2 - 3 that obtains in any of the irradiated Nb specimens. [The increase in ξ/a_o^3 at constant b with increasing κ is almost exactly balanced by the decrease in $1/\mu_{eff}$.] Therefore if we compare Q at constant reduced magnetic induction b for samples of differing κ we are making the comparison at a constant FLL compliance. We have chosen to make the comparison at b = .55 which is a low enough b to be below the complications of the peak effect near B_{c_2} but high enough to permit the normal high field approximations for computing μ_{eff} and f_p to be used. Furthermore, since F_p for most samples varies slowly with B in this range, the comparison is insensitive to small errors in defining B_{c_2}.

To determine the effects of defect density on Q we first establish a value of $Q(Q_o)$ at a density of $10^{23}m^{-3}$. This value was chosen because all the low temperature experiments have experimental points at densities reasonably close to this one. We then plot in Fig. 9 the ratio of Q/Q_o vs. ρ on a log-log plot. The open triangles represent the cascade pinning experiments of Berndt et al.[15], the filled triangles the cascade pinning experiments of Brown[16] and the filled hexagons the Frenkel defect pinning experiments of Ullmaier et al.[7,8]. Remarkably the results which span about three decades of defect density appear to fall on a single universal curve. The decrease in Q/Q_o above $\rho = 5x10^{22}m^{-3}$ can be qualitatively understood based on a modification of a simple argument given by Ullmaier[61,7]. He makes the reasonable assumption that at high pin density the FLL is sensitive only

to fluctuations in pin density between neighboring volumes of superconductors and that for purposes of determining these fluctuations one should average over a volume of $\simeq\xi^3$. The average number $\langle n\rangle$ of pins in ξ^3 is $\rho\xi^3$ and the average difference $\langle\Delta n\rangle$ in the number of pins between neighboring volumes is $\sqrt{\rho\xi^3}$ but the increased proximity of defects to each other must eventually result in a decrease in the effective interaction energy of a single defect with the FLL. If we make the very crude assumption that this decrease goes like the linear distance between defects $\rho^{-1/3}$ in this density range $f_p \propto \langle\Delta n\rangle(\rho)^{-1/3} \simeq$ constant and F_p will be given by $\xi^{-3} f_p$ or $\xi^{-3}Cf_p^2$ implying that for $\rho >> \frac{1}{\xi^3}$ Q goes asymptotically as $\frac{1}{\rho}$ is observed.

For our purposes however the most important aspect of Figure 8 is that it indicates that below a defect density of about 5×10^{22} the specific pinning force Q is independent of defect density. Note that the experimental range of void and dislocation loop densities mostly falls below this density so that we should expect Q to be a constant for a given size void or dislocation loop.* It will be possible to further test the independence of Q for voids in the next section.

We note in passing that the independence of Q at much smaller ρ's can be established in the case of precipitate pinning from the results of Antesberger and Ullmaier[62] who investigated pinning by Nb_2N particles in NbTa alloys over the density range $4\times10^{18}m^{-3}$ to $4\times10^{19}m^{-3}$ and the results of Bibby[63,1] who investigated pinning by 0.8μm diameter tungsten particles in Pb-Bi alloys over the range $1\times10^{17}m^{-3}$ to $5\times10^{17}m^{-3}$. While it would be very desirable to extend the range of density covered experimentally in Figure 8 and perhaps have more cascade points below $\rho \simeq 10^{23}m^{-3}$, we consider the proportionality between F_p and ρ, and the independence of Q on ρ, to be reasonably well established in this region.

---

* This statement clearly is not true for the smallest dislocation loops which have a very high ρ. We could use Fig. 8 to correct the Q for this density dependence. Since the correction does not significantly change the eventual conclusions we will ignore it in what follows.

Dependence of the Specific Pinning Force on Defect Size and Type:

The specific pinning forces for the defect conditions listed in Table I were computed at b = .55. For dislocation loops and voids the specific pinning force should be a strong function of the loop or void diameter and the results shown on Figure 10 bear out this expectation. As the dislocation loop diameter increased from 25Å to 160Å, the specific pinning force increases almost three orders of magnitude from 10^{-17} N to 10^{-14} N. Similarly for an increase in void diameter from about 50 to 500A, Q increases from just over 10^{-15} N to just under 10^{-11} N. The open circle void data represent the neutron irradiated samples whereas the filled circles represent the Ni^{+} ion irradiated specimens. Note that although the void densities differ by about one order of magnitude for comparable void diameters (Table I), there is excellent agreement between the two sets of data, providing one more indication that Q is indeed independent of density over the range of void density. The specific pinning force for Frenkel pairs and cascades are also shown although the "diameter" in these cases is not well defined. The downward arrow in each case represents the decrease in Q with increasing density shown in Fig. 9. In comparing theory with experiment one would choose the largest Q value since this one will represent as close as one can come to the Q for isolated defects.

The Q values are useful for another reason. Since we have calculated Q for b = constant and thus at constant FLL compliance a comparison of Q values between one defect and another is meaningful. Thus we can conclude that a void is about 20 times more effective as a pinning center than a dislocation loop of the same diameter, that a cascade is about an order of magnitude less effective than a dislocation loop of roughly the same size, and that a Frenkel pair surprisingly is only about a factor of 3 less effective than a 25Å dislocation loop.* The

* In light of the result reported by Professor Schilling (previous paper) that interstitials are mobile and cluster at 4.2 K in Nb this result is less surprising.

specific pinning forces are useful in another way however. They make possible a very dramatic comparison between both summation models simultaneously. To make such a comparison it is first necessary to make estimates of the elementary interaction forces and this is the subject of the next section.

ELEMENTARY INTERACTION FORCES

There are a large number of possible mechanisms by which a defect can interact with the flux line lattice[2,3,4]. However in the case of small voids and dislocation loops the situation is reasonably clear cut and one can claim with some certainty to know what the pinning mechanism is. Before discussing each of these cases in detail, it is first necessary to discuss the structure of the FLL. In the Ginzburg-Landau-Abrikosov theory[64,65] the superconductor is described by an order parameter Ψ, the square of which is proportional to the density of superconducting electrons. If Ψ_o is defined as the order parameter in zero field at the temperature of interest and ψ is defined as Ψ/Ψ_o the reduced order parameter the solutions of the Ginzburg-Landau equations in the mixed state produce a periodic ψ with nodes at the vortex cores (flux line positions). We will let the symbol ω represent $|\psi^2|$ and show in Figure 11 a map of ω at $b = .8$ from the paper by Brandt[66]. At the core of each vortex is a region approximately the coherence length ξ in radius that is depleted in superconducting electrons but ω rises to a maximum value approximately midway between the vortex cores.

Dislocation Loops: Strain Field Interactions:

Accompanying this spatial modulation of ω are modulations with the same periodicity in the volume and the elastic constants of the crystal[2,67,68]. In the core of the flux line the crystal is slightly denser (by about 1 ppm in Nb) and stiffer (by about 100 ppm in Nb). The volume modulation gives rise to a

periodic stress field[2,69,70]. A defect such as a dislocation loop that produces a strain field in the crystal lattice will interact with the FLL via the interaction between that strain field and the stress field of the FLL (this is the so-called parelastic or first order interaction[72]). It is also possible for the defect to interact with the FLL via the dielastic or second order interaction[73] between the elastic modulus modulation of the FLL and the square of the strain field of the defect.

The first order interaction between a dislocation loop and the FLL was calculated by Kramer[70] and by Pande[73]. The dielastic interaction has also been calculated by Kramer[70] for the dislocation loop and it has almost the ssme dependence on loop diameter as the parelastic interaction. Since the parelastic interaction predicts an attractive interaction between an edge dislocation and a flux line core in agreement with direct experimental observations by Herring[74,2] it must be somewhat larger than the dielastic interaction. Accordingly we shall use the results of the parelastic calculation to determine f_p. Since the dielastic interaction is of opposite sign for a small interstitial loop (the loop is attracted to the flux line core by the parelastic interaction and repelled by the dielastic) the parelastic f_p will if anything be an overestimate of the true f_p for such loops and an underestimate of the true f_p for small vacancy loops.

A map of the interaction force for a dislocation loop in a plane perpendicular to the magnetic field is shown in Fig. 12. The crosses represent the positions of flux line cores and the contours represent the locus of all positions of the loop where it will experience the same total force. Because of the translational symmetry of the FLL, the force exerted by the loop is periodic with its position in the FLL. We will take the maximum value f_p of the interaction force to be its value at $x = a_o/4$, $y = 0$. The dependence of f_p on dislocation loop radius is

particularly simple as shown in Fig. 13 where numerical values are those for a dislocation loop in niobium[70,21]. For small loops f_p increases proportional to D^2 but reaches a maximum and reverses sign for larger loops (the magnitude of f_p only is plotted in this figure). Pande[73] has shown that this D dependence is given analytically by $DJ_1(\alpha k_o D)$ where α is a constant, $k_o = 2\pi/a_o$ and J_1 is a Bessel function of order one. It is to be emphasized that the D^2 dependence of f_p for loops is a property of the disk-like symmetry of the loop and is independent of the detailed interaction mechanism.

Voids: Core Interactions:

While there is room for doubt about the relative magnitudes of the two strain field interactions with the FLL, the interaction mechanism of small voids with the FLL is clear[2,3,24]. If we consider an isolated vortex and create a small void in the superconductor far from the vortex where $\omega = 1$, we must destroy superconductivity in the volume V of the void and so lose the superconducting condensation energy $\frac{1}{2}\mu_o H_c^2 V$. On the other hand if the void is at the vortex center $\omega = 0$ and there is no energy penalty. Clearly there will be an attractive interaction between a void and a vortex core with an energy of interaction $E_{int} = \frac{1}{2}\mu_o H_c^2 V$. Since ω rises to 1 at about one coherence length from the isolated vortex core, the elementary interaction force f_p is approximately

$$f_p \simeq \tfrac{1}{2}\mu_o Hc^2 V/\xi \qquad (12)$$

This expression is used by Freyhardt[24] to compute the order of magnitude of f_p for voids. He found this core pinning interaction to be much larger than the parelastic or dielastic interaction between the stress field of a void due to its intrinsic surface stress or the stress field due to possible depletion or accretion of solute from or to the void surface. It can also be argued that for small voids any perturbation of the magnetic field (and thus the magnetic energy)

of the system which takes place over the penetration depth must be very small. Any magnetic interaction for a small void will be smaller than the core interaction. To compute the void interactions with the core in the flux line lattice the local free energy function proposed by Campbell and Evetts[2] can be used.

$$E = \tfrac{1}{2}\mu_o H_c^2[\xi^2\nabla^2\omega - \omega^2] + \tfrac{1}{2}\mu_o h^2 \tag{13}$$

where h is the local field. We find as do Campbell and Evetts that the most important term is $\tfrac{1}{2}\mu_o H_c^2 \xi^2 \nabla^2\omega$. The vortex lattice has lower energy if the void is at points of positive curvature of ω, i.e., the vortex cores [see Figure 11], than in between the voids where there is negative curvature. If we represent the void by a function $V(\underset{\sim}{r}')$ which is 1 inside the void and zero outside of it, the interaction energy as a function of position $\underset{\sim}{r}$ in the FLL is given by the integral

$$E_{int} = -\tfrac{1}{2}\mu_o Hc^2\xi^2 \int[V(\underset{\sim}{r}')\nabla^2\omega(\underset{\sim}{r}-\underset{\sim}{r}')]d\underset{\sim}{r}' \tag{14}$$

This integral may be evaluated using Fourier transforms as shown previously[4] and differentiating to find the interaction force we arrive at

$$f_x = \tfrac{1}{2}\mu_o H_c^2(1-b)\frac{A}{2}[\sin k_o(x - \tfrac{y}{\sqrt{3}}) + \sin k_o(x + \tfrac{y}{\sqrt{3}})] \tag{15a}$$

$$f_y = \tfrac{1}{2}\mu_o H_c^2(1-b)\frac{A}{2\sqrt{3}}[\sin k_o(x - \tfrac{y}{\sqrt{3}}) - \sin k_o(x - \tfrac{y}{\sqrt{3}}) + 2\sin\tfrac{2k_o y}{\sqrt{3}}] \tag{15b}$$

where $A = \frac{8\pi}{9}\xi^2 k_o^3 \frac{D^2}{g_1}\sqrt{\frac{\pi}{g_1 D}}J_{3/2}(g_1 D/2)$. Here $k_o = 2\pi/a_o$, g_1 is the magnitude of the primitive reciprocal lattice vector of FLL (g_1 equals $2k_o/\sqrt{3}$ and $J_{3/2}(g_1 D/2)$ is the Bessel function of order 3/2. If we evaluate the interaction force at $x = a_o/3$, $y = 0$ as before we find

$$f_p = \tfrac{1}{2}\mu_o H_c^2(1-b)A \tag{16}$$

Equations 15a and 15b for the void gives the same interaction force map shown previously for the dislocation loop [Fig. 12] as indeed will any defect with radial symmetry about the magnetic field direction[70]. It is also obvious from Eq. 5

that the interaction force oscillates with the periodicity of the FLL; the defect produces alternating positive and negative forces as it moves through the FLL. For very small voids Eq. 16 reduces to

$$f_p = \frac{4}{9} \xi^2 k_o^3 \mu_o H_c^2 (1-b) V \tag{17}$$

This is essentially the same expression found by Campbell and Evetts[2] and at b = .55 it gives results within a factor of 1.3 of the values computed from Eq. 13 by Freyhardt[24] and Koch et al.[25] for an isolated vortex. The dependence of f_p on void diameter is shown in Figure 14. The elementary interaction force increases as D^3 corresponding to Eq. 17 for small D but then reaches a maximum and decreases, actually changing sign at D ≈ 1000Å [only the magnitude of f_p is shown on Figure 14]. The decrease of f_p to zero [corresponding to the zeros of $J_{3/2}(g_1 D/2)$] has a simple physical interpretation. At certain void diameters which depend on the FLL spacing a_o, when a vortex core leaves the void, another one enters the void and there is no net change in energy. None of the voids in the experiments discussed are this large but the f_p for some of the largest voids must be decreased somewhat from the value predicted by Eq. 17. Finally, it should be emphasized that the f_p computed for small voids from the core interaction must be considered to be the most accurately known of all the elementary interactions. Its magnitude computed here should not be more than a factor of two removed from the correct value. Certainly there is no question that it is proportional to the volume of the void as long as the void is small.

In passing we note that one can compute the core interaction with a small disk or cylinder shaped void or precipitate oriented normal to the field directions using the same method as above. Equations 15-17 hold if A is now given by

$$A = \frac{8\pi}{9} \xi^2 k_o^3 \frac{\pi t D \, J_1(g_1 D/2)}{g_1} \tag{18}$$

where J_1 is the Bessel function of order 1, t is the thickness of the disk (or length of the cylinder) in the field direction and D is the disk diameter. How to compute the elementary interaction forces for the cascades and Frenkel pairs is much more uncertain although attempts at order of magnitude calculations have been made[15,16,7]. We will defer discussion of the f_p's for these defects until after we have compared the summation models with experiment using the void and dislocation loop data which will be the subject of the next section.

COMPARING SUMMATION MODELS WITH EXPERIMENT

We first make a plot of specific pinning force versus dislocation loop diameter and place on this plot lines which represent the two summation models, i.e., $Q = f_p$ for direct summation and $Q = Cf_p^2$ for the statistical summation. For Nb at b = .55 and 4.2K, $C \simeq 1.2 \times 10^{9} N^{-1}$. The results are shown in Figure 15 and demonstrate that although the dislocation loop specific pinning force depends approximately on f_p as f_p^2 as predicted by the statistical theory, the magnitude of Q is about three orders of magnitude larger than predicted by the theory. At the larger dislocation loop sizes especially the magnitude of Q is closer to that predicted by the direct summation. Even more disturbing we observe that if Q continues to increase as f_p^2 it will apparently cross and become greater than the direct summation line at a dislocation loop diameter greater than 500Å. As a final jarring disagreement between the statistical theory and experiment we note that by combining Eq. 6 and Eq. 11 we can determine the value of Q that will satisfy the threshold criterion, i.e.

$$Q_{min} = 4C \mu_{eff}^2 a_o^4. \tag{19}$$

For niobium at 4.2K and b = .55, $Q_{min} \simeq 2.5 \times 10^{-12} N$. A glance at Fig. 15 reveals the experimental Q values are from 5 to 2 orders of magnitude smaller than Q_{min}. In this range the statistical theory predicts that we should measure Q = 0.

Figure 15 shows the corresponding plot of Q versus D for voids. The dependence of f_p on D is D^3, not D^2 as in the dislocation loop case. The data do not run parallel to either the f_p or the Cf_p^2 line over the whole range of void diameters. Rather for small voids the dependence seems to be approximately as the 3/2 power of f_p with the power decreasing to something close to one for the larger voids. As in the case of the dislocation loops the magnitude of the specific pinning force is between the predictions of the two models and is somewhat more closely predicted by the direct summation than by the statistical theory. Also as in the case of the dislocation loops most of the specific pinning forces lie below the threshold criterion and all of the calculated elementary interaction forces lie below the threshold criterion using f_p as a basis (Eq. 6).

Before attempting to modify either of these theories to account for the experimental data we must first have confidence that these data are correct, particularly the f_p values. We can in fact make a consistency test with the data at hand since the f_p's for the dislocation loops and those for voids arise from two totally different mechanisms and since the Q values of the large dislocation loops and for the small voids overlap (e.g., Fig. 10). If both computations of f_p are correct a plot of specific pinning force versus f_p should yield a single master curve. Such a plot is displayed in Fig. 17. The superposition between the two sets of data both in terms of slope and magnitude is close to being perfect. One can now think of this master curve as the experimental solution to the summation problem, a solution that corresponds to neither the statistical theory or the direct summation. At low f_p's it parallels the statistical theory (there is a hint that it becomes even steeper at the lowest f_p's) but is displaced upward from the Cf_p^2 line by about 3 orders of magnitude. At higher f_p's it curves to a progressively smaller slope until at the highest f_p's it runs parallel to the direct summation line and achieves a magnitude that is only a factor 3 to 4 below

the magnitude of the specific pinning force predicted by the direct summation.

How accurately do we know the f_p's on this master curve? I will argue that we know them now accurately indeed. Since we know that the largest possible interaction mechanism for small voids is core pinning and since all calculations of the core pinning f_p give essentially the same answer, we know the f_p for the small voids rather well. Since the large dislocation loop Q's and f_p's overlap those of the small voids we must also have computed the magnitude of the stress field interaction between the large dislocation loop and the FLL accurately. Finally once one point on either the dislocation loop f_p vs D curve (Figure 13) or the void f_p vs D curve (Figure 14) is established, computing the f_p for another void or loop is simply a matter of determining the geometry of the defect and scaling approximately as D^3 for the void or D^2 for loop. Thus the points for the larger voids and smaller loops are accurately determined as well. A last consistency check is that none of the specific pinning force points lie above the direct summation line. But note that if the master curve in the void regime had not bent over to a lower slope but instead had followed the extrapolation of the dislocation loop data, the f_p's for the largest voids would have exceeded the direct summation by at least an order of magnitude.

DISCUSSION OF SUMMATION MODELS

It is now appropriate to discuss where the summation models go wrong and in what directions we should go to find a theory which can account for the empirical summation master curve. Since it is not difficult to think of many reasons why the curve should fall below the direct summation line, let us concentrate on the statistical theory of Labusch. We will find that the f_p^2 dependence of F_p is in fact an artifact of the pinning potential curve Labusch chose. Let

us start by observing from Fig. 17 that the true range of validity of the Labusch theory is strictly limited. Strictly speaking it cannot apply below the threshold criterion or an f_p of 4×10^{-11} N in niobium and it certainly cannot apply above an f_p of 10^{-9}N because an extension of the Cf_p^2 curve will bring it above the direct summation which is clearly impossible.* The f_p^2 dependence Labusch obtains is intimately connected with the threshold criterion and his choice of a potential function to represent interaction energy between the pin and the flux line lattice. He chose a single potential well for which the energy was zero for $|x| > \sqrt{3}$ d where d is an interaction distance from the center of the well. When this function is differentiated to obtain the force of the defect on the FLL, the f versus x curve has one positive-going maximum and one negative-going minimum and then goes to zero for large $|x|$. Somewhat more simple wells are considered by Ullmaier[3] and Lowell[77]; both derive the same f_p^2 dependence. Such a force (and energy) curve cannot correctly represent the interaction of the defect with the FLL since E and f are periodic functions with the periodicity of the FLL (see Fig. 12). Such a one dimensional periodic well is shown schematically in Figure 18a along with the f vs. x curves derived from it as the strength of the interaction is progressively increased (Fig. 18b, c, d). The potential is chosen such that the f vs x curves are simple triangular functions for simplicity but that choice is not essential to the argument. Let us place the well at an initial random position x_o with respect to the FLL and then turn on the interaction[78]. The FLL will be displaced by a displacement u according to the equation

$$k u = f + \left.\frac{df}{dx}\right|_{x_o} u \tag{20a}$$

or

$$u = \frac{f\big|_{x_o}}{k - \left.(df/dx)\right|_{x_o}} \tag{20b}$$

---

* Labusch[57] in fact recognized this upper limit and developed a "fluid approximation" for a highly distorted flux lattice which changes the u_{eff} in Eq. 6.

where k is the spring constant of the FLL (Eq. 7). As long as $|k|>|df/dx|$ everywhere one can always find an initial position x_o so that the FLL is displaced to any arbitrary position x_1 with respect to the defect. Since the well is symmetric with respect to x = 0, in the final state with a large number of randomly initially positioned pinning centers there will be just as many positive as negative force interactions in the displaced position and the total integrated force F_p will be zero. Such a well is below the threshold criterion and is shown in Fig. 18b where the slope of the dashed line represents k. If $|k|>|\frac{df}{dx}|$ as in Fig. 18c there will be a region of the well where the FLL cannot come to rest. Assume a FLL is being pushed to the left (-x direction) by the Lorentz force. If for a particular defect the maximum f is exceeded the FLL immediately jumps to a new position represented by the intersection of the dashed line with the f(x) curve. No FLL position between the peak force and that intersection is stable. Consequently an integration of the force provided by the well over all possible stable FLL positions results in a net positive force. The integration is from some minimum force f_{min} determined by the intersection to the maximum force. In the single potential well used by Labusch this minimum force cannot be positive and for $\frac{df}{dx} >> k$ this leads to $F_p \propto f_p^2$. For a periodic well however f_{min} can be greater than zero (see Fig. 18d) and in fact approaches f_p for $\frac{df}{dx} >> k$. Under these circumstances $F_p \propto f_p$. If we proceed to analyze the problem in detail as outlined in Ullmaier's book[3, p. 58-60] we find that Q for the potential of Fig. 18 is given by

$$Q = f_p^2(f_p-f_t)/(f_t+f_p)^2 \qquad (21)$$

where f_t is the threshold f_p (for this $f_t = k a_o/4 = \pi a_o^2 \mu_{eff}$). On the other hand using a single well as Labusch did we get

$$Q = Cr_p^2(f_p-f_t)(f_p+3f_t)/(f_p+f_t)^2 \qquad (22)$$

Plotting these two functions on a graph of Q versus f_p we get the curves shown on Figure 19. The correct solution for the periodic well rises steeply above the threshold and then becomes asymptotic to the direct summation for an f_p about one order of magnitude above the threshold. There is no extended region over which F_p is proportional to f_p^2! Although the general shape of this curve is similar to the experimental master curve the approach of the master curve to a line approximately parallel to the direct summation is much more gradual and takes place over at least three decades in f_p, Figure 17. Also we are still left with the fact that the threshold f_p would have to be displaced down to at least below 10^{-15}N.

One possibility that can be discarded is that the recalculation of the FLL elastic constant by Brandt will produce enough displacement of the threshold to account for the discrepancy. Schmucker and Brandt[41] have redetermined μ_{eff} using Brandt's theory and the line representing the recalculated μ_{eff} for Nb at b = .5 and 4.2°K is shown in Figure 16. There is only a small change in μ_{eff} and a small shift of the threshold criterion at this b; at larger b however the difference is much greater.

Another possible way to circumvent the threshold criterion is the one first suggested by Fietz and Webb[43]. They argued that perhaps groups of elementary pins should be considered as superpinning centers. To move the threshold down 5 orders of magnitude would require the bundling of 10^5 defects into a single supercenter. Such a pin would have dimensions so large it could no longer be considered a point pinning center[21,24]. It is also difficult to imagine such a mechanism giving rise to a Q that is independent of pin density on a master curve.

The most realistic possibility is that FL dislocations in FLL increase the effective compliance of the FLL so as to permit the threshold criterion to be fulfilled[78]. If we consider a one dimensional model of the FLL (Figure 20) we can think of nearby dislocations as weak springs in that chain of vortices. The bowing out of the dislocation in response to f_p will give a spring constant k which is inversely proportional to the dislocation loop length squared and directly proportional to the line tension of the dislocation which in turn is proportional to $\sqrt{C_{66}C_{44}}$ [79]. Thus the stiffness of this "weak spring" would essentially have the same magnetic field and temperature dependence as μ_{eff} of the perfect FLL. Furthermore since different pins will be at different distances from dislocations, the effective k will vary greatly and some pins will be above threshold while some will be below. As f_p is increased the approach to the direct summation will be rather gradual as observed. Finally the FL dislocation hypothesis offers a way to explain flux lattice history effects on F_p[30-32]. Interestingly Küpfer and Gey[32] find that very strong pins do not show flux lattice history effects. This observation now can be understood since these are already almost to the direct summation line and their contribution will not be affected much by increasing the FL dislocation density and thus lowering the threshold f_p. While much work remains to be done to make this FL dislocation hypothesis a quantitative model I believe that it is the most promising theoretical direction in which to seek the answer to the low threshold criterion.

Finally it should be noted that any relaxation of the elastic constraints present in the infinite FLL will have the same effect as introducing a weak spring. In particular the presence of a free surface parallel to the flux line should have the effect of drastically decreasing the effective k for the FLL at pins near the surface. There is considerable evidence in the literature[80-83] which suggests that defects near a surface are more effective in pinning (have

larger Q's than those in the bulk). Our group at Cornell has done an experiment in which we neutron irradiated triangular Nb prisms at room temperature to form dislocation loops and measured the anisotropy of the critical current with respect to the angle between the magnetic field direction and one of the faces of the prism. The size of the current peak when the field is parallel to the face is an indication of the surface contribution to the critical current. As illustrated in Figure 21 we found that the irradiation increased the height of the surface current peak above the background bulk critical current as well as the breadth of the peak. Since irradiation does not change other properties of the surface such as roughness this result directly proves that dislocation loops near the surface are more effective in pinning flux than those in the bulk. The probable reason for this is the decrease in the threshold criterion and the increase in Q caused by the relaxation of the elastic constraints on the FLL due to the presence of the nearby surface.

EXPERIMENTAL IMPLICATIONS OF A MASTER CURVE FOR SUMMATION

If the summation master curve in Figure 17 is to be generally useful it should be able to be applied to defects other than dislocation loops and voids. Hence it is important to check to see if quantitative experiments other than the irradiation experiments fit on the curve. Unfortunately such experiments where both f_p and ρ are well known are rare. One such experiment is the experiment of Lippmann, Schelten and Schmatz[84] who measure F_p and ρ for large normal precipitates of Nb_2N in Nb. Their value of Q at b = .55 together with their estimate of f_p is included on Fig. 17 as the open triangle. It is evident that this point lies near the continuation of the master curve as well as almost directly on the

line representing the Cf_p^2 approximation to the statistical theory of Labusch.*

The data of Antesberger and Ullmaier on flux pinning by Nb_2N precipitates in $Nb_{.73}$-$Ta_{.27}$ also fits. Although μ_{eff} is decreased slightly from its value for Nb the shift of the Cf_p^2 line in Fig. 17 is only to just above the line labelled Schmucker and Brandt. The Q values determined from their measurements on samples with $\rho = 4.7 \times 10^{19} m^{-3}$, $1.7 \times 10^{17} m^{-3}$ and $4 \times 10^{18} m^{-3}$ are $Q = 1.4 \times 10^{-12} N$, $1.8 \times 10^{-12} N$ and $1.5 \times 10^{-12} N$ respectively at b = .55. The f_p values estimated for their precipitates are about $10^{-11} N$ which puts their points well above the Cf_p^2 line and in good agreement with the points for the larger voids on the master curve.†

Finally there are a number of experiments on flux pinning by dislocations in deformed Nb[86-88]. Theoretically the f_p between a perpendicular dislocation and the FLL is $\simeq 10^{-13} N$ about the same as for a large dislocation loop whereas the f_p values extracted from the data using the Labusch analysis are at least one order of magnitude higher implying a $Q \simeq 10^{-15} - 10^{-14} N$ which is close to the master curve.

---

* They also measured $\langle f^2 \rangle$ by measuring the mean square displacement $\langle u^2 \rangle$ of a flux line from neutron diffraction experiments and converting to $\langle f^2 \rangle$ using Eq. 5. They found good agreement between the calculated f_p and $\langle f^2 \rangle^{\frac{1}{2}}$. Because the $\langle u^2 \rangle^{\frac{1}{2}}$ measured are greater than $a_o/3$ for this large precipitate it is not clear whether the presence of FL dislocations and their effect on the k would be detected by this experiment. Neutron diffraction experiments on the weakly pinning dislocation loop samples would be very useful in deciding why the threshold criterion is fulfilled.

† Based on experiments on single crystal Nb samples containing disk-shaped precipitates of diameter D and thickness t, Antesberger and Ullmaier[85] have claimed that only a Cf_p^2 summation will explain the F_p difference measured between the situation when the field is parallel to a <100> direction and when it is parallel to a <111> direction. Such a claim is in fact based on a miscalculation of f_p which in this situation is proportional to the maximum cross-sectional area of the particle on a plane perpendicular to the direction of motion of the flux lattice. Proceeding to do the averaging the same way they do, I find that $f_{p_{100}} \propto \langle L_{z_{100}} \rangle \langle L_{100} \rangle \propto D^2/2$ whereas $f_{p_{111}} \propto \langle L_{z_{111}} \rangle \langle L_{111} \rangle \propto .8Dt/\sqrt{3}$. The ratio $f_{p_{100}}/f_{p_{111}}$ is 1.08 D/t. Since the observed D/t ratios are 8-10 a linear summation which is indicated by the results of large voids can account for their measured ratios $F_{p_{100}}/F_{p_{111}} \simeq 8$.

Let us then use this experimental master summation curve to estimate the elementary interaction forces between the FLL and the other irradiation-produced defects, i.e., cascades and Frenkel pairs. From Fig. 10 we find a maximum Q value for dilute cascades of about 3×10^{-16}N. On the master curve this value of Q corresponds to an f_p value of 10^{-14}N. For the most dilute array of Frenkel pairs $Q \simeq 5\times10^{-18}$N. If we extend the master curve slightly we see that this value of Q corresponds to an f_p of about 2×10^{-15}N. It is difficult to make theoretical estimates for f_p for either of these defects but one can make crude attempts. For example one might consider the ∿650 atom depleted zone in the center of a 3 MeV cascade to be an incipient void and calculate the pinning expected from a void of 650 atoms with a volume $1.2\times10^{-26}m^3$. The f_p for such a void is $\simeq5\times10^{-15}$N which is within a factor of two of the experimentally determined value. The interaction energy due to the dielastic interaction between an isolated vortex and a Frenkel defect has been estimated by Ullmaier et al.[7] to be $E = \varepsilon_b \Delta Y/Y$ where ε_b is the elastic energy of a Frenkel pair which they set a 5eV and $\Delta Y/Y$ is the change in Young's modulus between the superconducting and normal state in Nb ($\Delta Y/Y \simeq 10^{-4}$). Following the methods outlined above f_p can be established to be $f_p = k_o E_{int}(1-b)/2$. Using the numbers for Nb $f_p \simeq 10^{-15}$N in reasonable agreement with the value of 2×10^{-15}N determined from Q and the master curve.

CONCLUSIONS

It is apparent that flux pinning experiments in irradiated superconductors have provided and will continue to provide important clues as to the correct form of summation models. The advantages of such experiments are that they allow the introduction of single, well characterized defect species that approximate point pinning centers. The low temperature irradiations allow the introduction of various numbers of defects with a constant size distribution to test the density

dependence of summation whereas higher temperature irradiations allow the introduction of dislocation loops and voids of controlled size for which f_p can be accurately estimated. The results to date indicate that the pinning force density is proportional to point pin density below pin densities of $5 \times 10^{22} m^{-3}$ and that at moderate reduced magnetic field (b = .5) neither the direct summation nor the statistical theory of Labusch are satisfactory summation models. Rather it has been shown that an empirical master summation curve can be constructed which is parallel or just below the direct summation at high f_p but decreases approximately as f_p^2 at low f_p. Extending this master curve to other reduced fields and temperatures should be a high priority objective of both future experiments and theoretical investigations.

Acknowledgements:

I wish to acknowledge stimulating discussions with Dr. J. E. Evetts, Dr. H. C. Freyhardt and Professor D. N. Seidman. I also thank Dr. Freyhardt, Dr. E. H. Brandt, Dr. H. A. Ullmaier, Dr. H. Küpfer and Professor E. Saur for sending me preprints of their work prior to publication. Financial support for writing this review was provided by the U.S. Office of Scientific Research under grant AFOSR-77-3107 while the experiments on dislocation loop pinning described herein were supported by the U.S. Energy Research and Development Administration. This work also benefited from the use of the facilities of the Cornell Materials Science Center which is funded by the National Science Foundation.

REFERENCES

1. J. D. Livingston and H. W. Schadler, Prog. Mater. Sci. 12 (1964) 183.

2. A. M. Campbell and J. E. Evetts, Adv. in Physics 21 (1972) 199.

3. H. Ullmaier, Irreversible Properties of Type II Superconductors, Springer Tracts in Mod. Physics 76 (1975).

4. E. J. Kramer, J. of Electronic Materials 4 (1975) 839.

5. D. C. Agrawal, B. D. Lauterwasser and E. J. Kramer, Materials Sci. and Engineering 21 (1975) 125.

6. J. Auer and H. Ullmaier, Phys. Rev. B7 (1973) 136.

7. H. Ullmaier, K. Papastaikoudis, S. Takács and W. Schilling, Phys. Stat. Sol. 41 (1970) 671.

8. H. Ullmaier, K. Papastaikoudis, S. Takács and W. Schilling, Proceedings of the 12th International Conference on Low Temperature Physics, Kyoto, Japan (1970) p. 309.

9. T. H. Blewitt, M. A. Kirk and T. L. Scott, Proceedings of Conference on Fundamental Aspects of Radiation Damage in Metals, Gatlinburg, TN, Oct. 1975, to be published.

10. D. N. Seidman, Radiation Damage in Metals, Ed. N. L. Peterson and S. D. Harkness, ASM (1976) p. 28.

11. K. L. Merkle, Radiation Damage in Metals, Ed. N. L. Peterson and S. D. Harkness, ASM (1976) p. 58.

12. B. S. Brown, Radiation Damage in Metals, Ed. N. L. Peterson and S. D. Harkness, ASM (1976) p. 330.

13. M. T. Robinson and I. M. Torrens, Phys. Rev. B, 9 (1974) 5008.

14. G. H. Kinchin and R. S. Pease, Rep. Progress in Phys. 18 (1955) 1.

15. H. Berndt, N. Kartascheff and H. Wenzl, Z. f. Angew. Phys. 24 (1968) 305.

16. B. S. Brown, Proc. International Discussion Meeting on Flux Pinning in Superconductors (IDMFPS), ed. P. Haasen and H. C. Freyhardt (Akademie der Wissenschaften, Göttingen, 1975) p. 200.

17. R. H. Kernohan and S. T. Sekula, J. Appl. Phys. 38 (1967) 4904.

18. S. T. Sekula, J. Appl. Phys. 42 (1971) 16.

19. C. A. M. van der Klein, P. H. Kes and D. de Klerk, Phil. Mag. 29 (1974) 559.

20. B. A. Loomis and S. B. Gerber, Acta Met. 21 (1973) 165.

21. D. C. Agrawal, E. J. Kramer and B. A. Loomis, Phil. Mag. 33 (1976) 343.

22. R. W. Rollins and Y. Anjaneyulu, J. Appl. Phys. 48 (1977) 1296.

23. D. I. R. Norris, Radiation Effects 14 (1972) 1; 15 (1972) 1.

24. H. C. Freyhardt, Radiation-Induced Flux Pinning in Type II Superconductors, Institut für Metallphysik, Universität Göttingen (1976).

25. C. C. Koch, H. C. Freyhardt and J. O. Scarborough, Proc. of 1976 Applied Superconductivity Conference, Stanford (1976), to be published.

26. B. A. Loomis, A. Taylor and S. B. Gerber, J. Nuclear Materials 56 (1975) 25.

27. A. B. Pippard, Phil. Mag. 19 (1969) 217.

28. E. J. Kramer, J. Appl. Phys. 44 (1973) 1360.

29. E. J. Kramer, Proceedings of I.D.M.F.P.S. (see Ref. 16) p. 240.

30. M. Steingart, A. Putz and E. J. Kramer, J. Appl. Phys. 44 (1973) 5580.

31. R. W. Rollins, H. Küpfer and W. Gey, Proc. of I.D.M.F.P.S. (see Ref. 16) p. 142; J. Appl. Phys. 45 (1974) 5392.

32. H. Küpfer and W. Gey, to be published in Phil. Mag.

33. B. D. Lauterwasser and E. J. Kramer, Phys. Letters 53A (1975) 410.

34. R. Schmucker, Phys. Stat. Sol. (b) 80 (1977) 89.

35. E. H. Brandt, Communications in Physics 1 (1976) 57.

36. E. H. Brandt, J. Low Temp. Phys. 26 (1977) 709.

37. E. H. Brandt, J. Low Temp. Phys. 26 (1977) 735.

38. E. H. Brandt, J. Low Temp. Phys. 28 (1977) to be published.

39. E. H. Brandt, J. Low Temp. Phys. 28 (1977) to be published.

40. R. Labusch, Phys. Stat. Sol. 32 (1969) 439.

41. R. Schmucker and E. H. Brandt, Phys. Stat. Sol.(b) 79 (1977) 479.

42. K. E. Osborne and E. J. Kramer, Phil. Mag. 29 (1974) 685.

43. W. A. Fietz and W. W. Webb, Phys. Rev. 178 (1969) 657.

44. R. A. Brand, Ph.D. Thesis, Cornell University, 1972.

45. M. P. Mathur, M. Ashkin, D. W. Deis and B. J. Shaw, IEEE Trans. Magn. MAG-11, (1975) 255.

46. M. R. Daniel, A. I. Braginski, G. W. Roland, J. R. Gavaler, R. J. Bartlett and L. R. Newkirk, J. Appl. Physics 48 (1977) 1293.

47. Private communication, E. J. Kramer to A. I. Braginski, Aug. 12, 1976.

48. J. Petermann, Z. Metallkunde 61 (1970) 724.

49. C. C. Koch and R. W. Carpenter, Phil. Mag. 25 (1972) 303.

50. O. Daldini, P. Martinoli, J. L. Olsen and G. Bernier, Phys. Rev. Letters 32 (1974) 218.

51. P. Martinoli, O. Daldini, C. Leemann and E. Stocker, Solid State Commun. 17 (1975) 205.

52. O. Daldini, C. Leemann and P. Martinoli, Solid State Commun. 16 (1975) 509.

53. P. Martinoli, O. Daldini, C. Leemann and B. van der Brandt, Phys. Rev. Letters 36 (1976) 382.

54. H. Raffy, E. Guyon and J. C. Reynard, Solid State Commun. 14 (1974) 427,431.

55. A. F. Hebard, A. T. Fiory and S. Somekh, Proc. of 1976 Applied Superconductivity Conference, Stanford (1976), to be published.

56. D. Dew-Hughes, Phil. Mag. 30 (1974) 293.

57. R. Labusch, Crystal Lattice Defects 1 (1969) 1.

58. K. Yamafuji and F. Irie, Phys. Letters A 25 (1967) 387.

59. J. Lowell, J. Phys. C 3 (1970) 712.

60. J. A. Good and E. J. Kramer, Phil. Mag. 22 (1970) 329.

61. H. A. Ullmaier, Proc. International Conf. on Defects and Defect Clusters in BCC Metals and their Alloys, Gaithersburg, MD, Aug. 1973, p. 363.

62. G. Antesberger and H. A. Ullmaier, Phil. Mag. 29 (1974) 1101.

63. G. W. Bibby, Ph.D. Thesis, Cambridge University, 1970.

64. V. L. Ginzburg and L. D. Landau, JETP 20 (1950) 1064.

65. A. A. Abrikosov, Sov. Phys. JETP 5 (1957) 1174.

66. E. H. Brandt, Phys. Stat. Sol. (b) 51 (1972) 345.

67. R. Labusch, Phys. Rev. 170 (1968) 470.

68. K. Miyahara, F. Irie and K. Yamafuji , J. Phys. Soc. Japan 27 (1969) 290.

69. G. Kluge and V. Rudat, Sov. Phys. JETP 38 (1974) 738.

70. E. J. Kramer, Phil. Mag. 33 (1976) 331.

71. E. J. Kramer and C. L. Bauer, Phil. Mag. 15 (1967) 1189.

72. W. W. Webb, Phys. Rev. Lett. 11 (1963) 191.

73. C. S. Pande, Appl. Phys. Lett. 28 (1976) 462.

74. C. P. Herring, Physics Letters 47A (1974) 105.

75. P. W. Anderson, Phys. Rev. Letters 9 (1962) 309.

76. J. Friedel, P. G. deGennes and J. Matricon, Appl. Phys. Lett. 2 (1963) 119.

77. J. Lowell, J. Phys. F 2 (1970) 547.

78. A similar, if not identical, model was developed by A. M. Campbell and J. E. Evetts and was presented by Dr. Evetts at the TMS-AIME Symposium on Superconducting Materials and Applications, Niagara Falls, Sept. 1976.

79. E. J. Kramer, J. Appl. Phys. 41 (1970) 621.

80. P. S. Schwartz and H. R. Hart, Jr., Phys. Rev. A 137 (1965) 818; Phys. Rev. 156 (1967) 412.

81. H. R. Hart, Jr. and P. S. Schwartz, Phys. Rev. 156 (1967) 403.

82. E. J. Kramer and A. Das Gupta, Phil. Mag. 26 (1972) 769.

83. A. Das Gupta and E. J. Kramer, Phil. Mag. 26 (1972) 779.

84. G. Lippmann, J. Schelten and W. Schmatz, Phil. Mag. 33 (1976) 475.

85. G. Antesberger and H. Ullmaier, Phys. Rev. Letters 35 (1975) 59.

86. H. C. Freyhardt, Phil. Mag. 23 (1971) 345.

87. H. C. Freyhardt, I.D.M.F.P.S. (see Ref. 16) p. 98.

88. W. Schlump and H. C. Freyhardt, I.D.M.F.P.S. (see Ref. 16) p. 129.

FIGURE CAPTIONS

Figure 1. Bright field transmission electron micrographs showing the dramatic increase in the density, and decrease in size of black spot (dislocation loop) radiation damage as the oxygen content (in wt. ppm) of niobium is increased.

Figure 2. Histograms of the density of dislocation loops of diameter D as a function of D determined from the electron micrographs of Figure 1 showing the change in the size distribution of the loops with oxygen content.

Figure 3. Global pinning force density F_p versus reduced magnetic induction for niobium irradiated with 3 MeV electrons at 4.2K from [7]. The curves represent different electron fluences and are labeled in terms of the resistivity increment $\Delta\rho$ produced by the irradiation: ◇, $\Delta\rho$ = 2.6nΩcm; □, $\Delta\rho$ = 5.4nΩcm; ○, $\Delta\rho$ = 17.5nΩcm; △, $\Delta\rho$ = 51nΩcm.

Figure 4. Global pinning force density F_p vs. reduced magnetic induction for niobium irradiated with fast neutrons at 4.6K from [15]. The curves represent different neutron fluences: ■, 7.1×10^{15}nvt; ●, 2.6×10^{16}nvt; □, 1.2×10^{18}nvt; ◇, 2.6×10^{18}nvt; ○, 4.7×10^{18}nvt.

Figure 5. Global force density F_p vs. reduced magnetic induction for niobium irradiated with fast neutrons at room temperature to a fluence of 9×10^{19}nvt from [21]. The curves represent different oxygen contents in wt. ppm: ◇, 904 ppm; □, 480 ppm; △, 250 ppm; ○, 10 ppm.

Figure 6. Global pinning force density F_p versus reduced magnetic induction for niobium irradiated with 3.5 MeV Ni^+ ions at elevated temperature from [24]. Curves represent different doses expressed in displacements per atom (DPA), irradiation temperatures T_{irr} and impurity content: ▽, 66 DPA, T_{irr} = 780°C, 140 ppm O; △, 83 DPA, T_{irr} = 780°C, 140 ppm O; ◇, 55 DPA, T_{irr} = 800°C, 140 ppm O; □, 61 DPA, T_{irr} = 785°C; ○, 130 DPA, T_{irr} = 865°C, 1 at % Zr, 570 ppm O.

Figure 7. Global pinning force density F_p versus reduced magnetic induction for niobium irradiated with a fast neutron fluence of $\sim 1 \times 10^{22}$ nvt (E > 1 MeV) from [25]. Curves represent samples irradiated at various elevated temperatures.

Figure 8. Global pinning force density F_p versus reduced magnetic induction b for the sample in Figure 6 irradiated at 800°C to 55 DPA. The curves represent different measuring temperatures: ▽, 8.5K; △, 6.5K; □, 4.9K; ◇, 4.2K; ○, 3.8K.

Figure 9. The ratio of the specific pinning force $Q = F_p/\rho$ to the $Q = Q_o$ at $\rho = 10^{23} m^{-3}$ plotted versus ρ.

Figure 10. The specific pinning force $Q = F_p/\rho$ plotted versus defect diameter D. For voids the open circles represent neutron irradiated samples while the closed circles represent Ni^+ ion irradiated samples. The downward arrows for Frenkel defects and cascades represent the trend of the data as the density of these defects is increased.

Figure 11. A map of ω, the square of the reduced order parameter for b = .8 from [66].

Figure 12. A contour map of the elementary interaction force f in arbitrary units between a dislocation loop (or any defect with radial symmetry about the field direction) as a function of the coordinate of the center of the loop. The crosses represent the position of vortex cores. Although only part of the unit cell of the FLL is shown the symmetry of the FLL can be used to obtain the fully periodic interaction force map.

Figure 13. The maximum elementary interaction force f_p for a dislocation loop in Nb at b = .55 and T = 4.2K evaluated at ($x = a_o/4$; $y = 0$) as a function of the loop diameter D.

Figure 14. The maximum elementary interaction force f_p for a void in Nb at b = .55 and T = 4.2K evaluated at ($x = a_o/4$; $y = 0$) as a function of the void diameter D.

Figure 15. The specific pinning force $Q = F_p/\rho$ versus dislocation loop diameter [21] in Nb at b = .55 and T = 4.2K. Lines representing the direct summation $Q = f_p$ and the statistical theory $Q = Cf_p^2$ are also drawn for comparison.

Figure 16. The specific pinning force $Q = F_p/\rho$ versus void diameter[24,25] in Nb at b = .55 at T = 4.2K. Lines representing the direct summation $Q = f_p$ and the statistical theory $Q = Cf_p^2$ are also drawn for comparison.

Figure 17. The specific pinning force $Q = F_p/\rho$ versus elementary interaction force f_p for defects in Nb at b = .55 and T = 4.2K. The open square represents the dislocation loop data[21], the open circles the data on voids [25] produced by neutron irradiation at high temperatures and the closed circles the data on voids produced by Ni^+ bombardment at high temperatures

[24]. The triangle represents data of Lippmann, Schelten and Schmatz[84] on large Nb_2N precipitates in Nb. Lines representing the direct summation $Q = f_p$ and the statistical theory of Labusch $Q = Cf_p^2$ are drawn together with a line representing the Labusch statistical theory using the recalculated FLL elastic constants from Schmucker and Brandt[41].

Figure 18. a) Periodic elementary interaction potential between a defect and the FLL as a function of distance x. b) Elementary interaction force versus x for the potential above. The slope of the dashed line represents the spring constant k of the FLL (see text). All FLL positions are stable. c) Effect of increasing f_p is that an instability develops and only positions between the intersection of the dashed line with the curve (minimum force) and f_p are stable. The threshold is exceeded. d) f_p is now well above threshold and the minimum force (intersection) is above zero. The increase of minimum force above zero will not occur for the single potential well used previously to represent the defect-FLL interaction.

Figure 19. Theoretical specific pinning force $Q = F_p/\rho$ vs f_p above the threshold f_p for a single well having a single period triangular force curve (Labusch theory), the Cf_p^2 approximation to that result, and the summation based on the periodic potential of Fig. 18a.

Figure 20. Simple schematic vortex and spring model of the deformation of the FLL showing the effect of weak springs (bowing out FL dislocations).

Figure 21. The surface contribution to the critical current of a triangular niobium prism as a function of the angle ϕ between the magnetic field and the surface. The different curves show the increase in this contribution with neutron irradiation at room temperature indicating that defects (dislocation loops) near the surface are more effective in pinning flux than those in the bulk.

TABLE I

Important Parameters of Irradiated Samples

Sample Identification	Reference	Defect Density ρ (m^{-3})	$Q = F_p/\rho$ (N)	Defect Size
Frenkel defects				
	[7]	1.5×10^{23}	5.4×10^{-18}	~5Å
	[7]	2.6×10^{23}	4.4×10^{-18}	~5Å
	[7]	5.3×10^{23}	2.7×10^{-18}	~5Å
	[7]	8.4×10^{23}	1.8×10^{-18}	~5Å
	[7]	1.5×10^{24}	1.1×10^{-18}	~5Å
	[7]	2.0×10^{24}	0.81×10^{-18}	~5Å
	[7]	2.5×10^{24}	0.64×10^{-18}	~5Å
Cascades				
1.1×10^{15} nvt	[15]	2.0×10^{21}	2.0×10^{-16}	80-150Å
2.6×10^{16} nvt	[15]	7.3×10^{21}	1.7×10^{-16}	80-150Å
1.4×10^{17} nvt	[15]	4×10^{22}	1×10^{-16}	80-150Å
1.2×10^{18} nvt	[15]	3.5×10^{23}	1.4×10^{-17}	80-150Å
2.6×10^{18} nvt	[15]	7.3×10^{23}	1.1×10^{-17}	80-150Å
4.7×10^{18} nvt	[15]	1.3×10^{24}	6.1×10^{-18}	80-150Å
3×10^{17} nvt	[16]	1×10^{23}	2.9×10^{-16}	80-150Å
5.4×10^{17} nvt	[16]	1.7×10^{23}	1.9×10^{-16}	80-150Å
8.6×10^{17} nvt	[16]	2.8×10^{23}	2.4×10^{-16}	80-150Å
2.7×10^{18} nvt	[16]	8.9×10^{23}	7.6×10^{-17}	80-150Å
3.7×10^{18} nvt	[16]	1.2×10^{24}	5.1×10^{-17}	80-150Å
Dislocation Loops				
10 ppm O	[21]	7.0×10^{21}	8.9×10^{-15}	165Å
250 ppm O	[21]	5.4×10^{22}	2.9×10^{-16}	60Å
480 ppm O	[21]	9.0×10^{22}	5×10^{-17}	30Å
904 ppm O	[21]	1.3×10^{23}	1.4×10^{-17}	25Å
Voids				
Ni^+ ion irradiated				
66 DPA, 780°C	[24]	4.1×10^{22}	6.1×10^{-15}	71Å
83 DPA, 780°C	[24]	3.0×10^{22}	3.9×10^{-14}	100Å
55 DPA, 800°C	[24]	3.6×10^{21}	4.9×10^{-13}	247Å
61 DPA, 785°C	[24]	3.4×10^{21}	7.3×10^{-13}	264Å
130 DPA, 865°C	[24]	1.4×10^{21}	3.6×10^{-12}	421Å
Neutron irradiated				
650°C	[25]	3.8×10^{22}	1.6×10^{-15}	47Å
790°C	[25]	1.7×10^{21}	2.4×10^{-13}	164Å
940°C	[25]	3.5×10^{20}	1.7×10^{-12}	283Å
1080°C	[25]	1.0×10^{20}	2.7×10^{-12}	461Å

Nb + OXYGEN IMPURITY

$9 * 10^{19}$ nvt (E > 0.1 MeV)

25°C

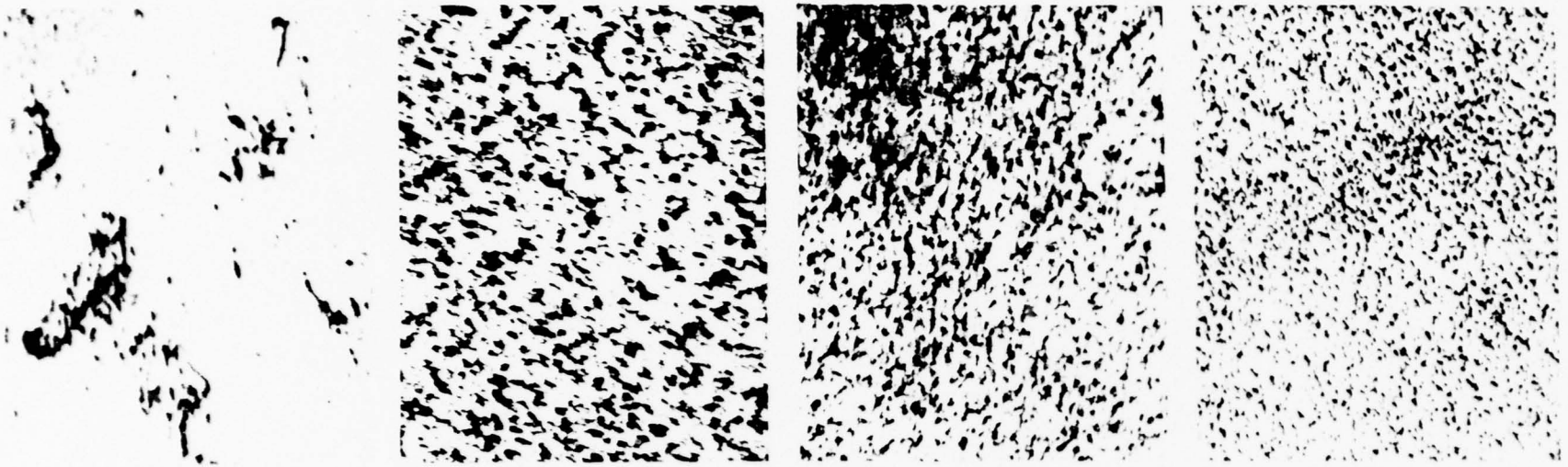

10 ppm 250 ppm 480 ppm 904 ppm

2000 Å

180,000 X

Fig. 1

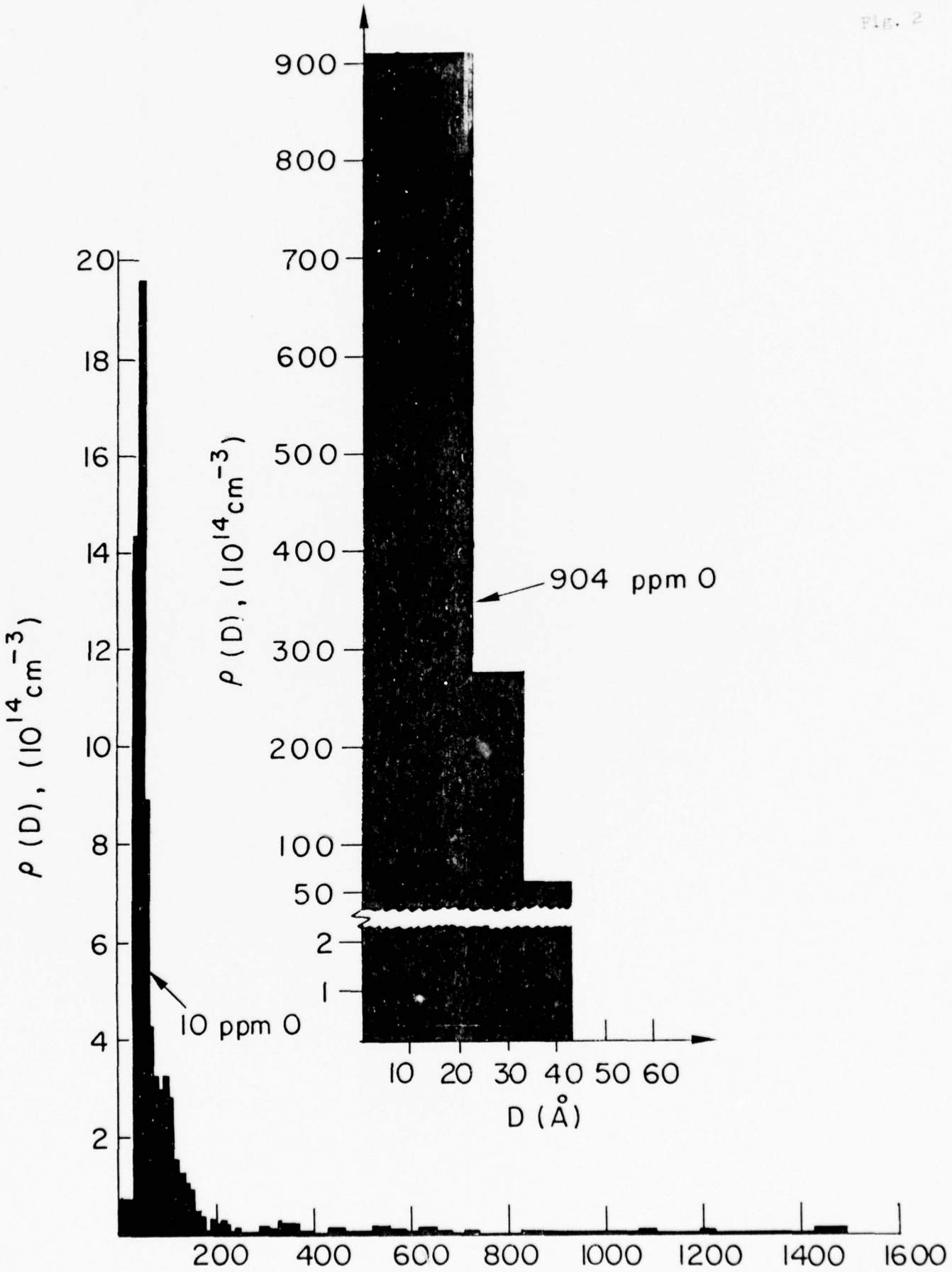
900
800
700
600
500
400
300
200
100
50
2
1
20
18
16
14
12
10
8
6
4
2
ρ (D), (10^14 cm^-3)
904 ppm O
10 ppm O
10 20 30 40 50 60
D (Å)
200 400 600 800 1000 1200 1400 1600

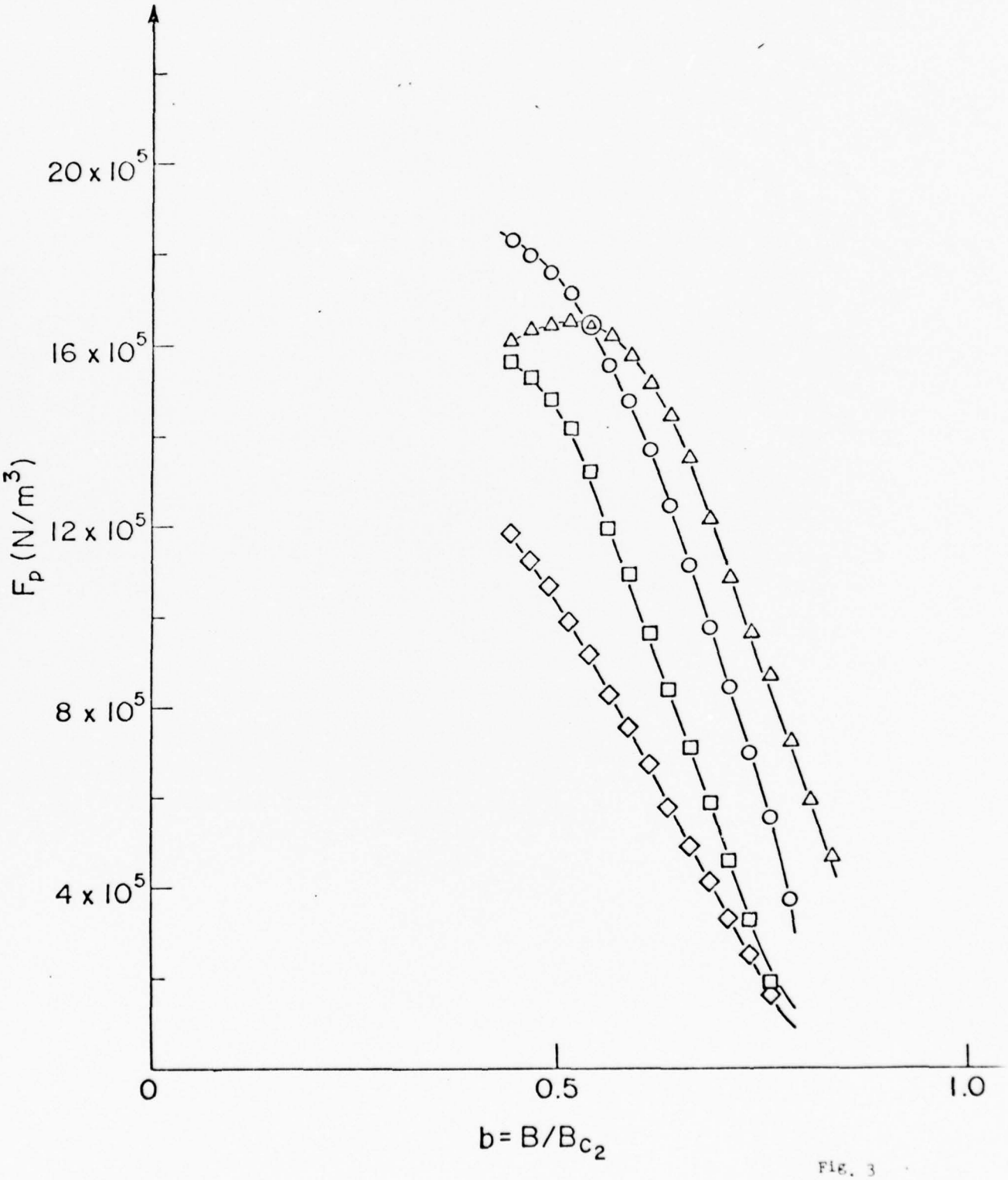

Fig. 3

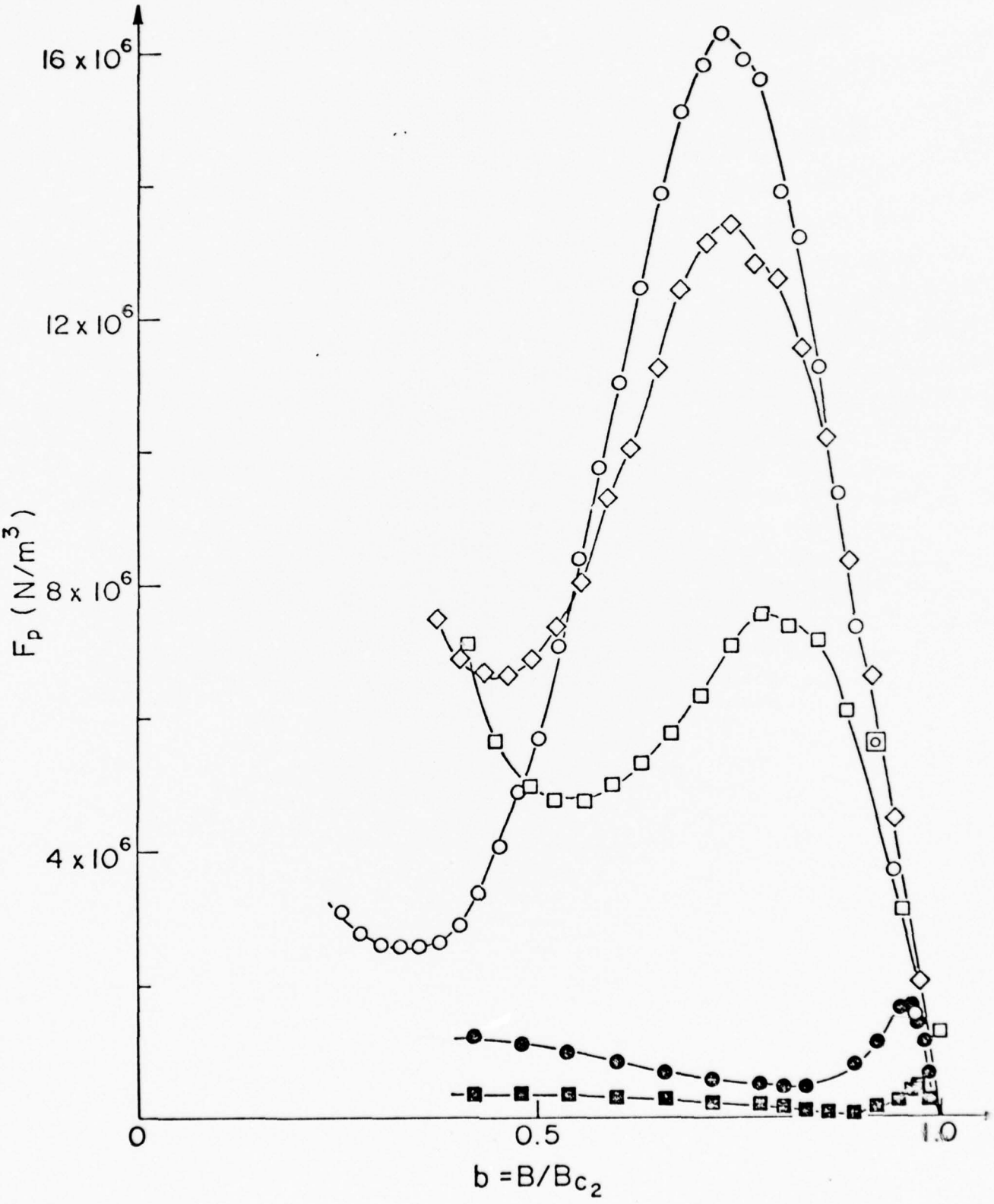

Fig. 4

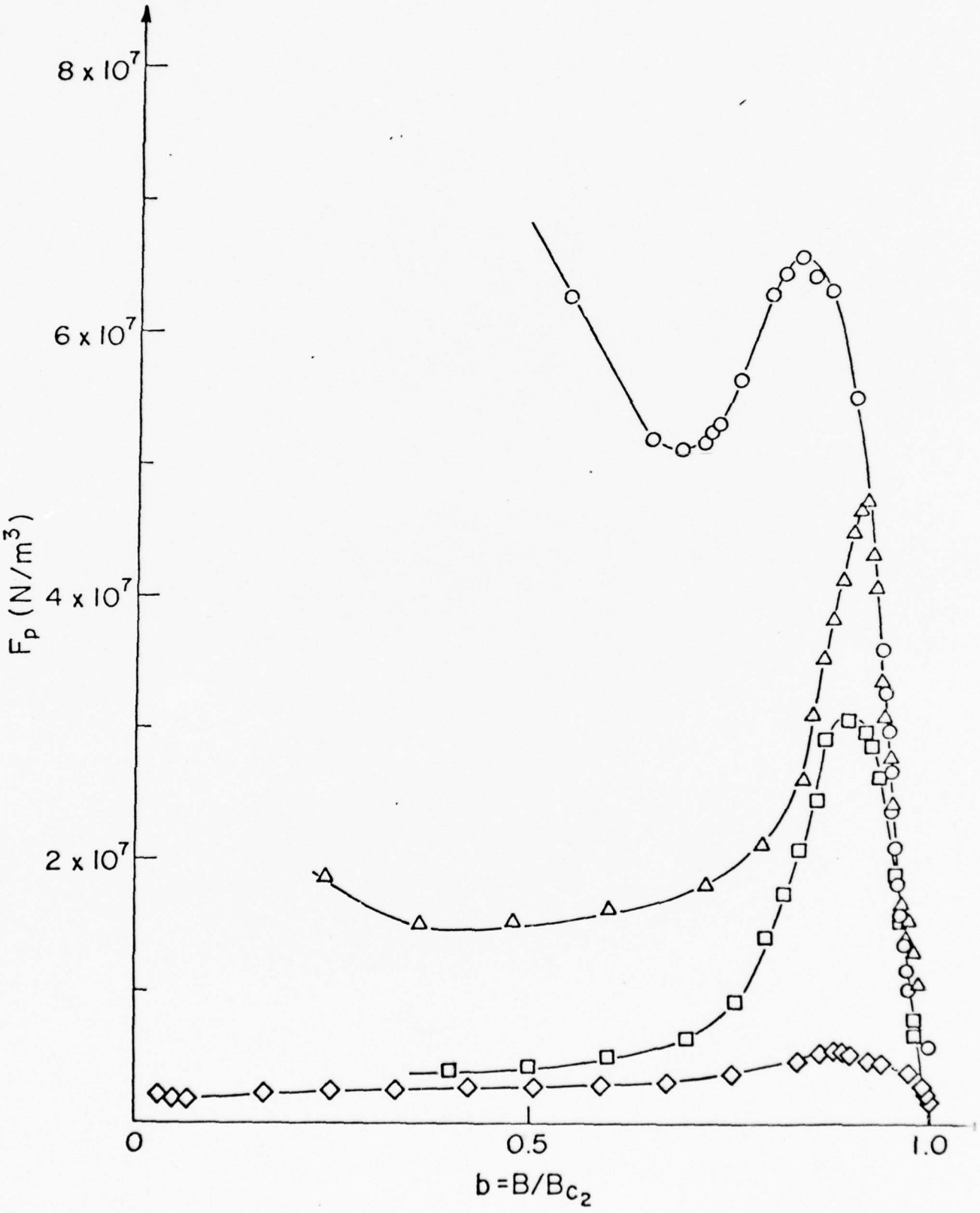

Fig. 5

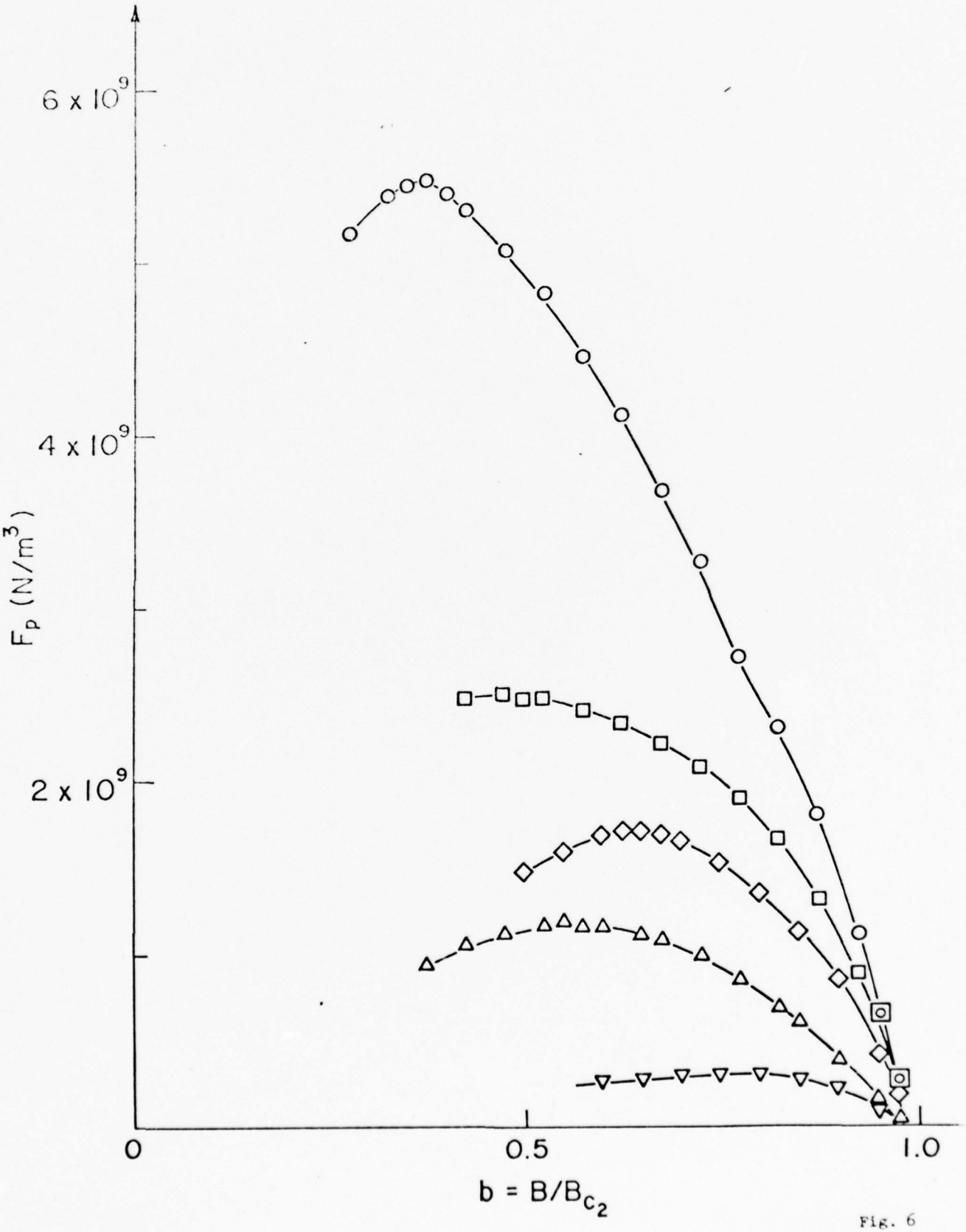

Fig. 6

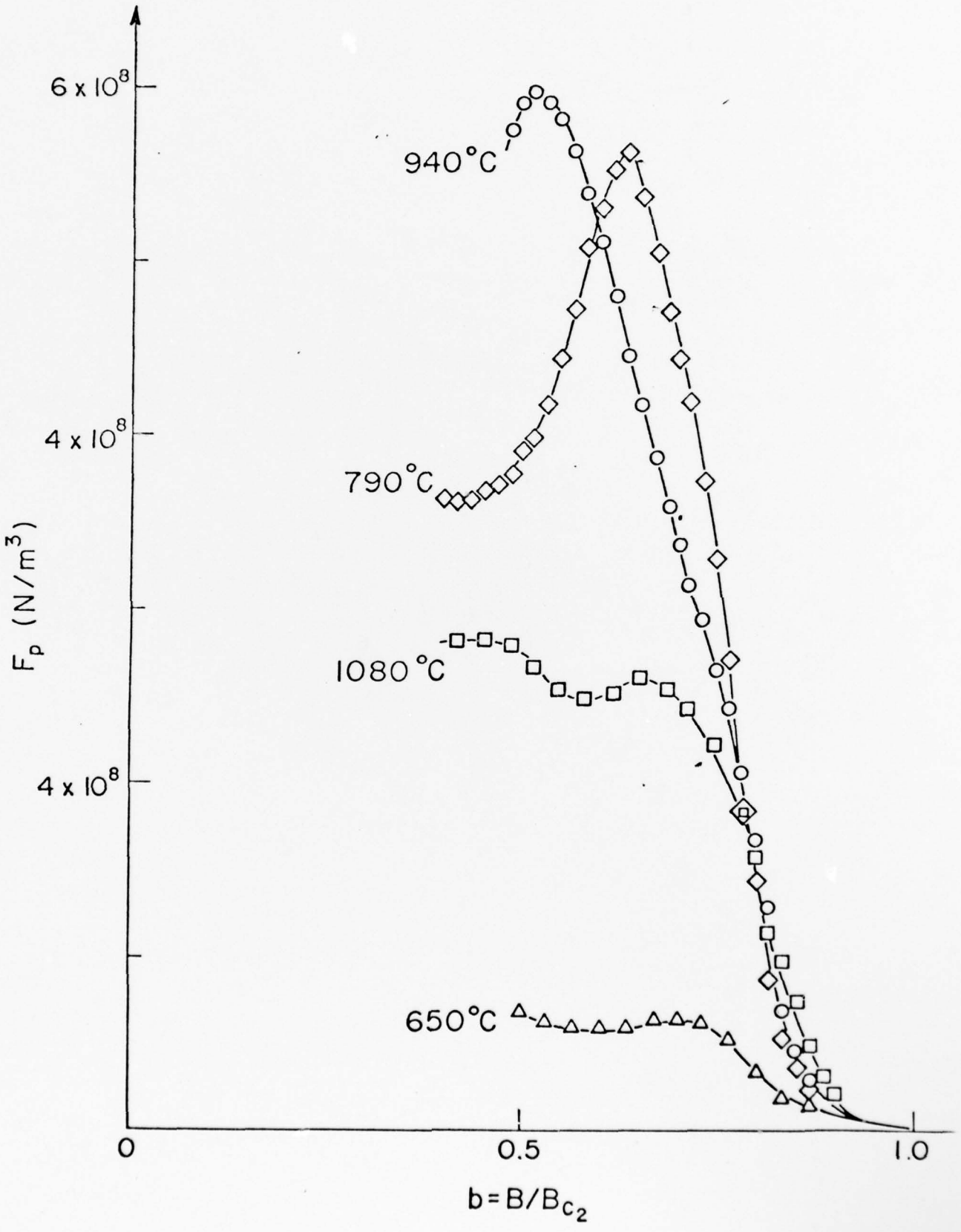

Fig. 7

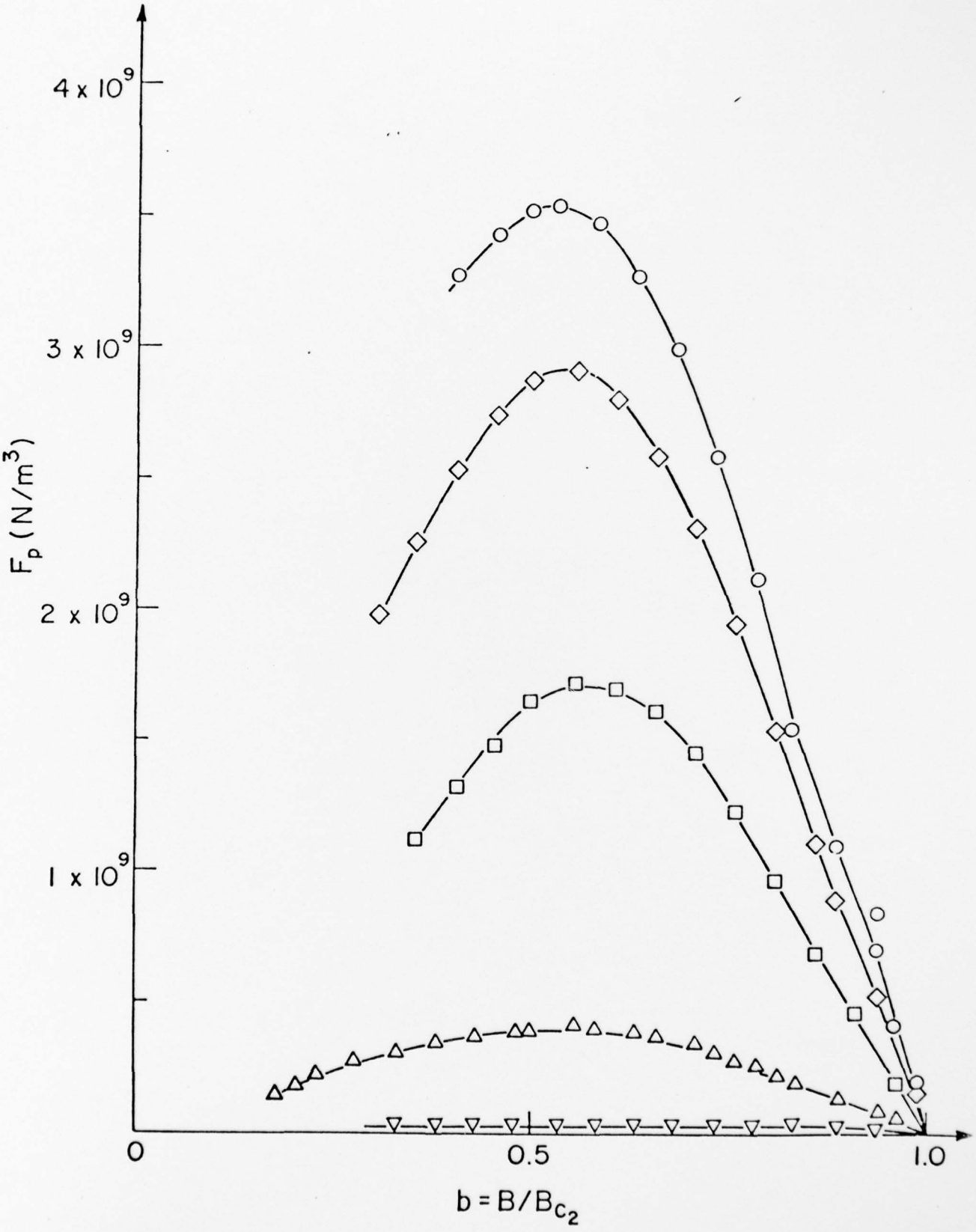

Fig. 8

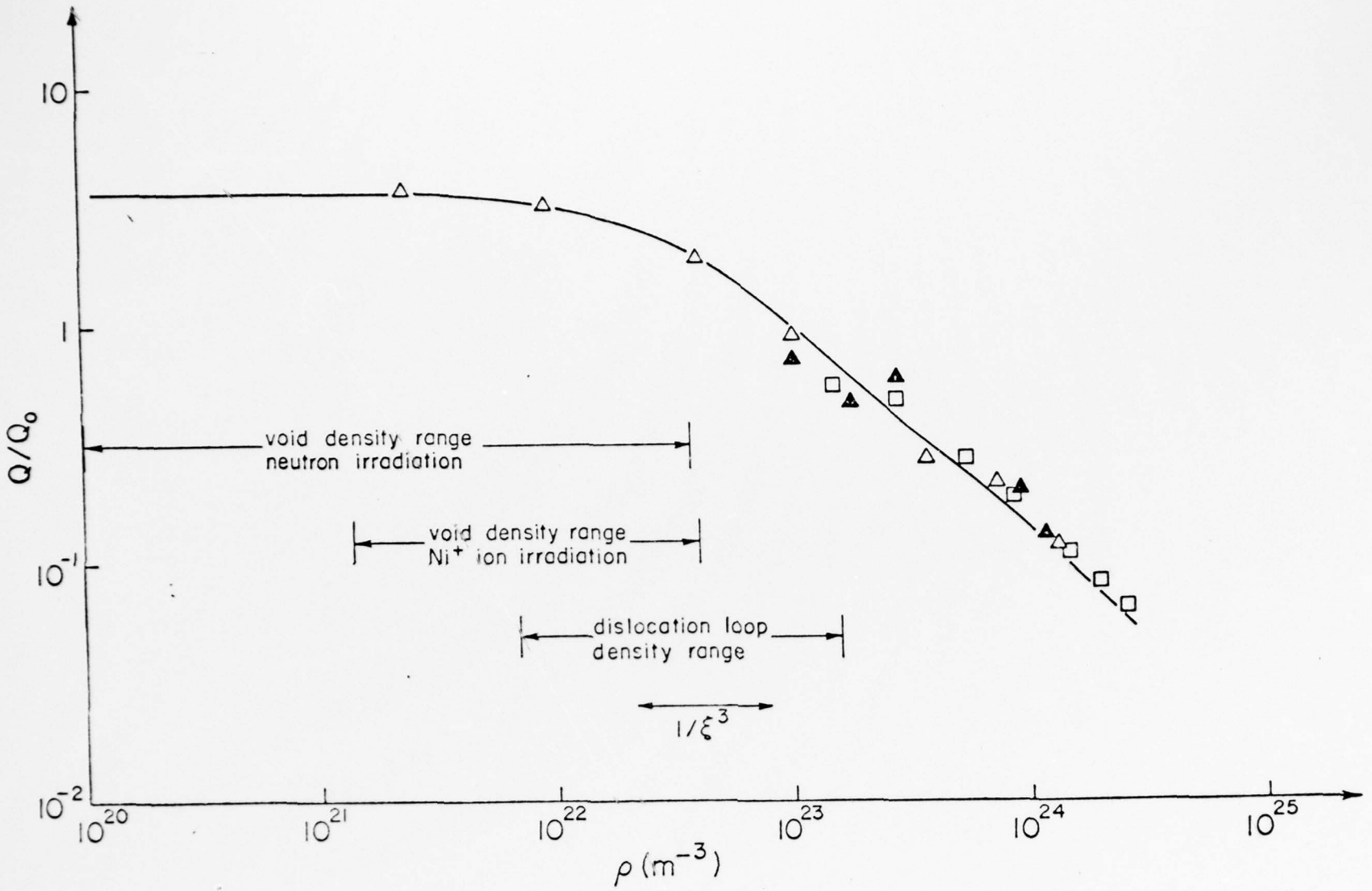
10
1
10^{-1}
10^{-2}
Q/Q_o
void density range
neutron irradiation
void density range
Ni^+ ion irradiation
dislocation loop
density range
$1/\xi^3$
10^{20}
10^{21}
10^{22}
10^{23}
10^{24}
10^{25}
$\rho\,(m^{-3})$

Fig. 9

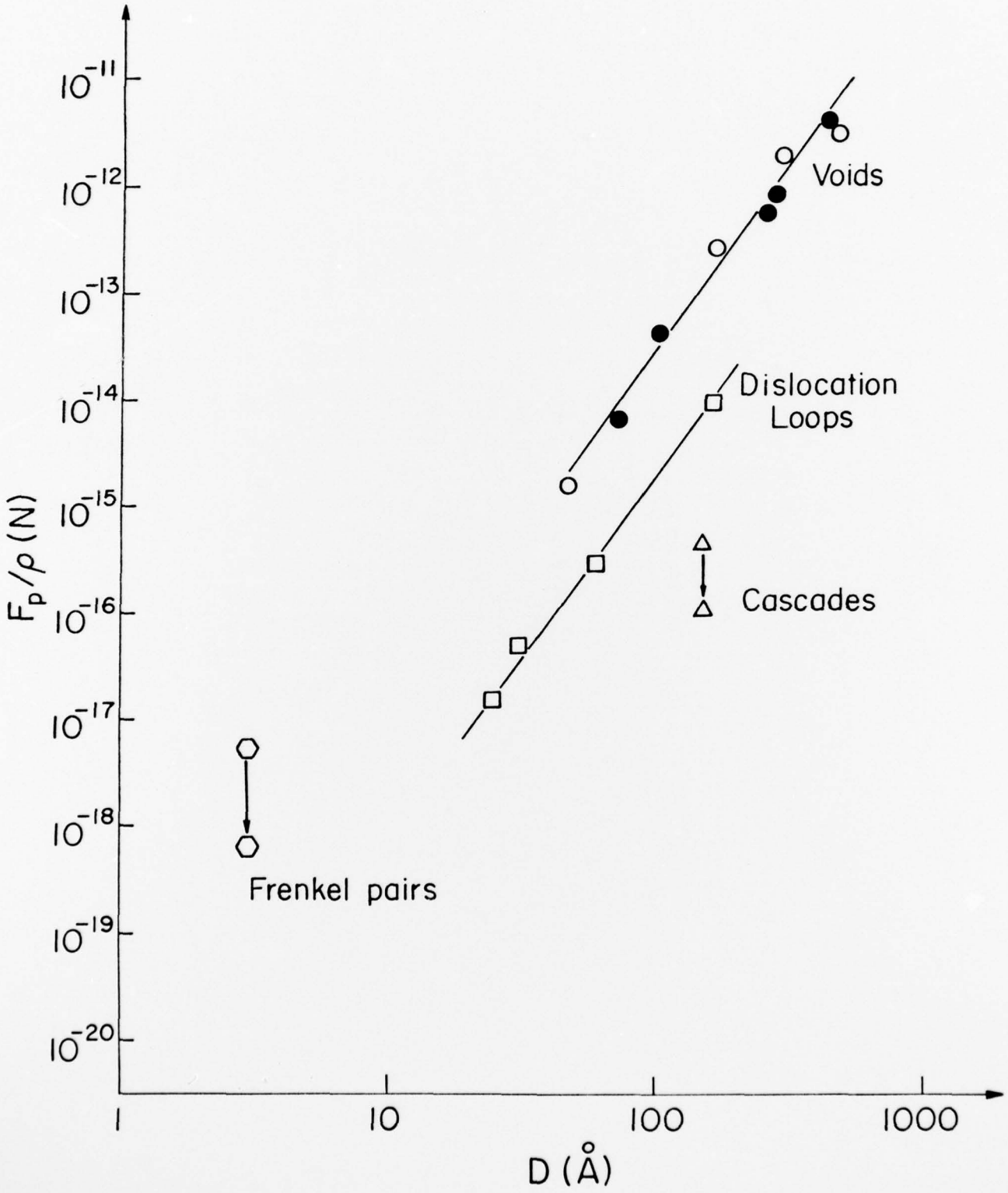
10^{-11}
10^{-12}
10^{-13}
10^{-14}
10^{-15}
10^{-16}
10^{-17}
10^{-18}
10^{-19}
10^{-20}
F_p/ρ (N)
Voids
Dislocation Loops
Cascades
Frenkel pairs
1
10
100
1000
D (Å)

Fig. 10

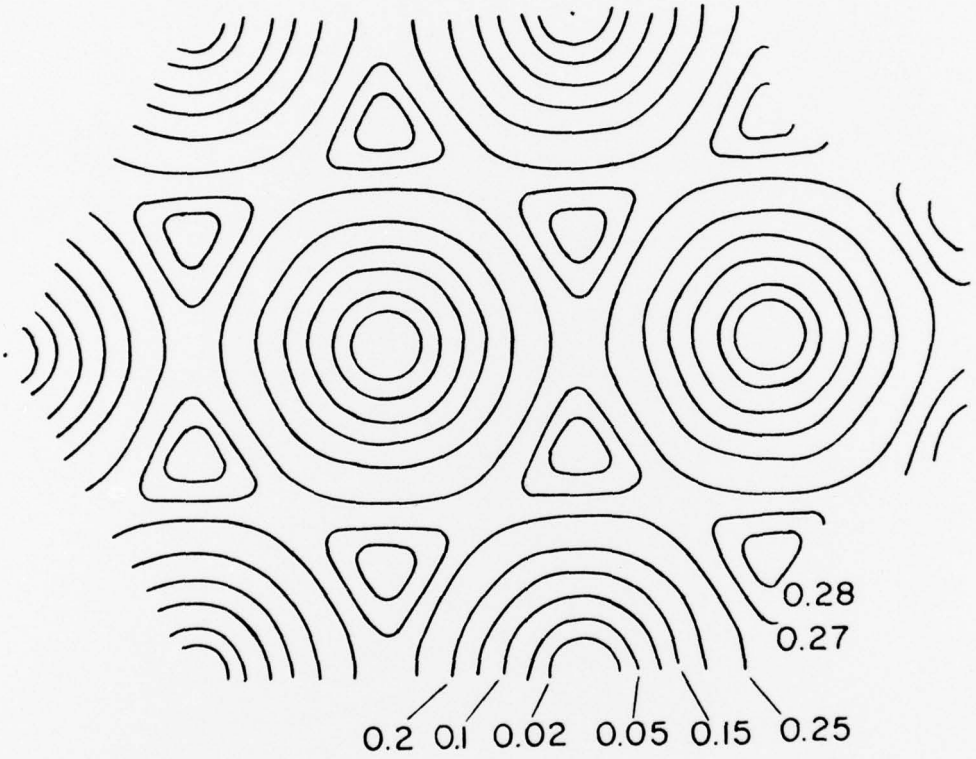

Fig. 11

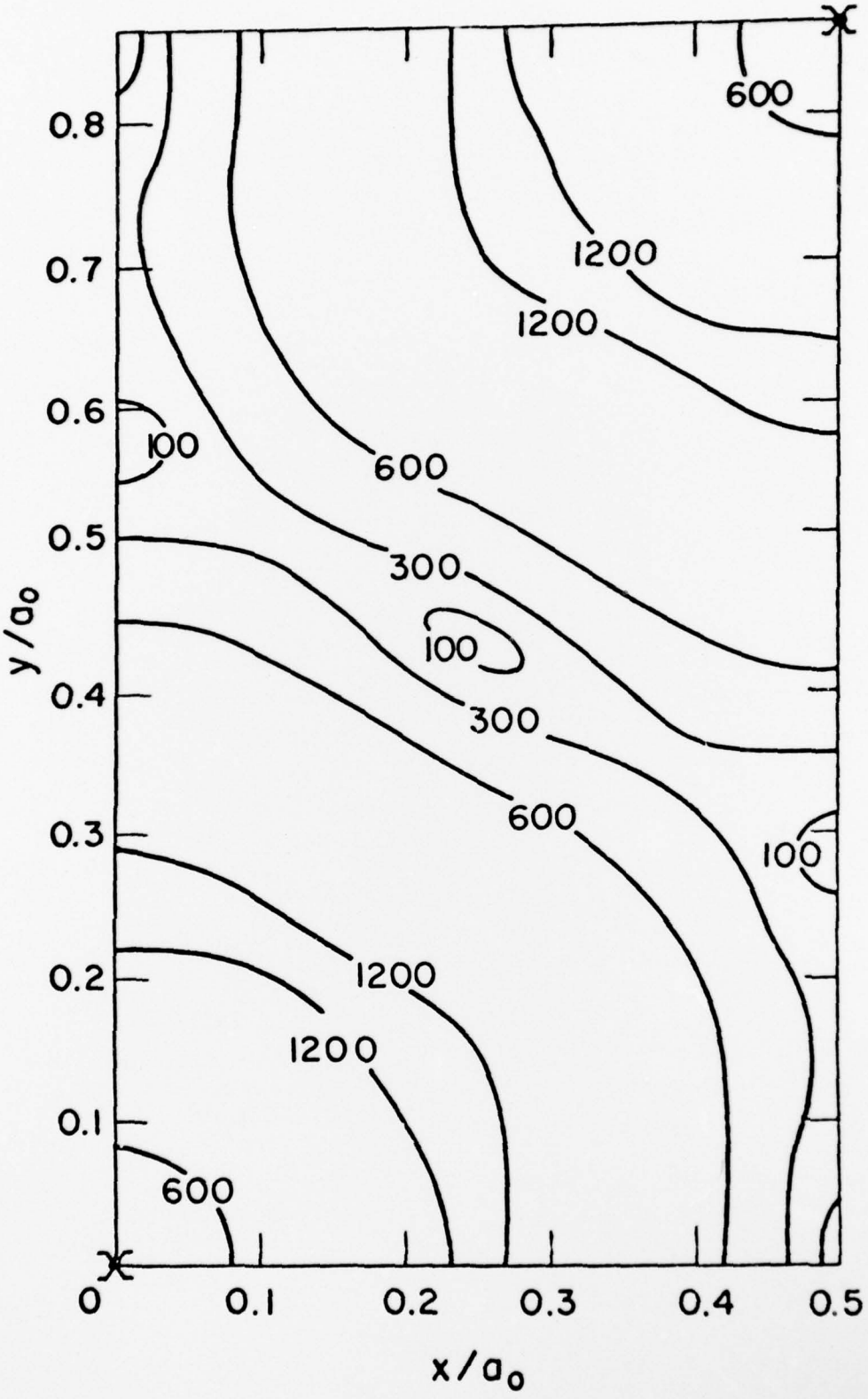
600
1200
1200
100
600
300
100
300
600
100
1200
1200
600
0.8
0.7
0.6
0.5
0.4
0.3
0.2
0.1
0
0.1
0.2
0.3
0.4
0.5
y/a0
x/a0

Fig. 12

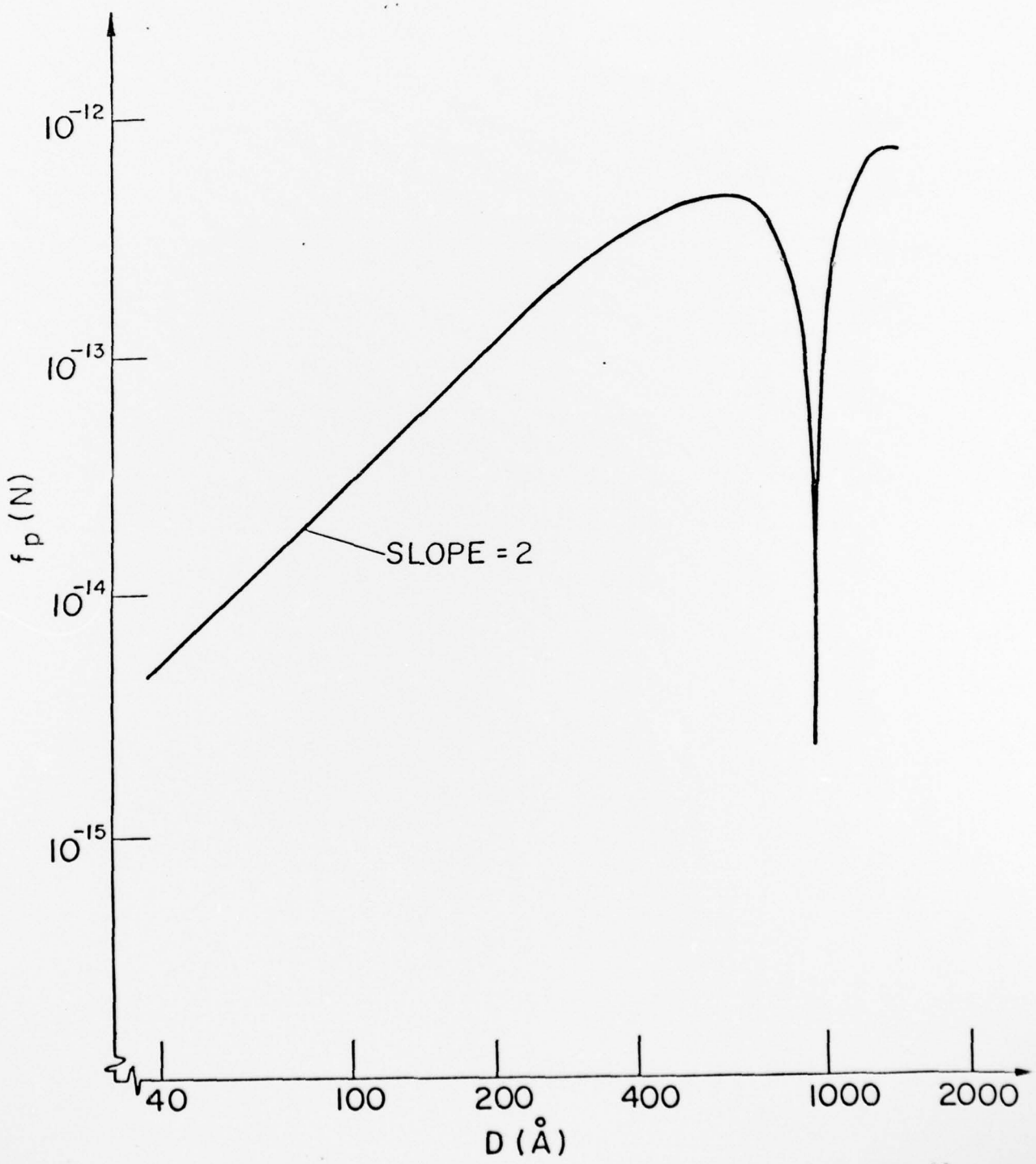

Fig. 13

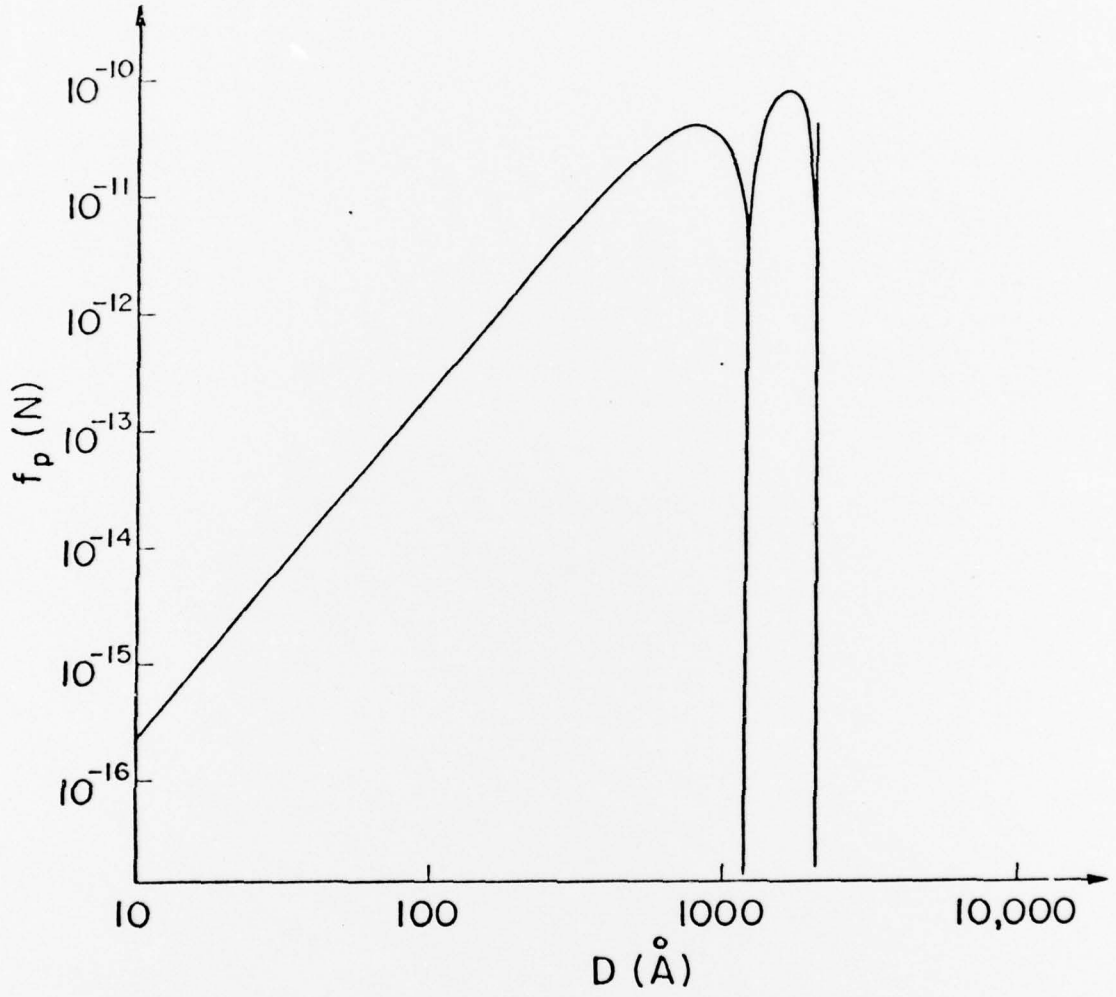

Fig. 14

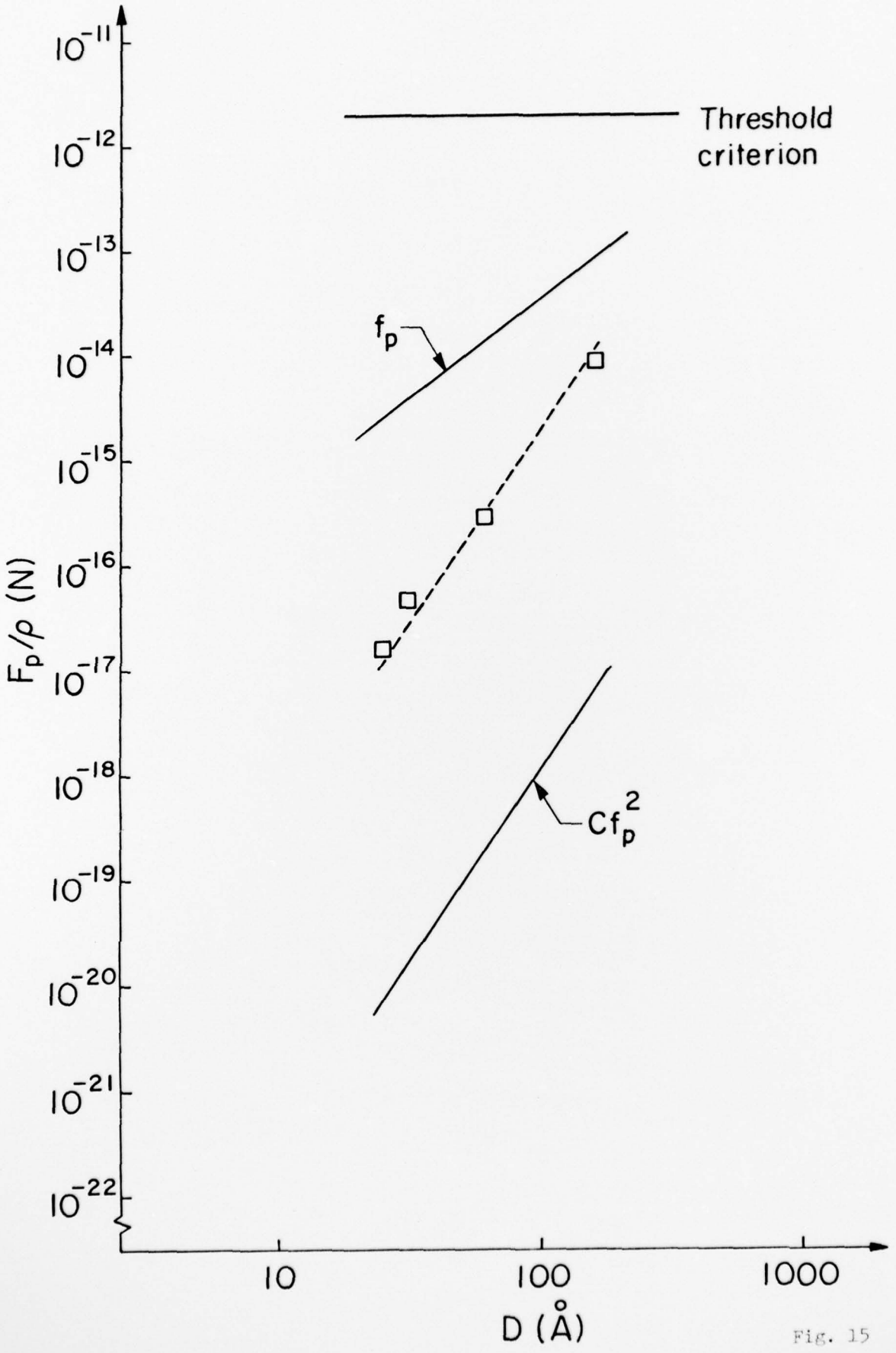
Threshold criterion
f_p
Cf_p^2
F_p/ρ (N)
10^{-11}
10^{-12}
10^{-13}
10^{-14}
10^{-15}
10^{-16}
10^{-17}
10^{-18}
10^{-19}
10^{-20}
10^{-21}
10^{-22}
10
100
1000
D (Å)

Fig. 15

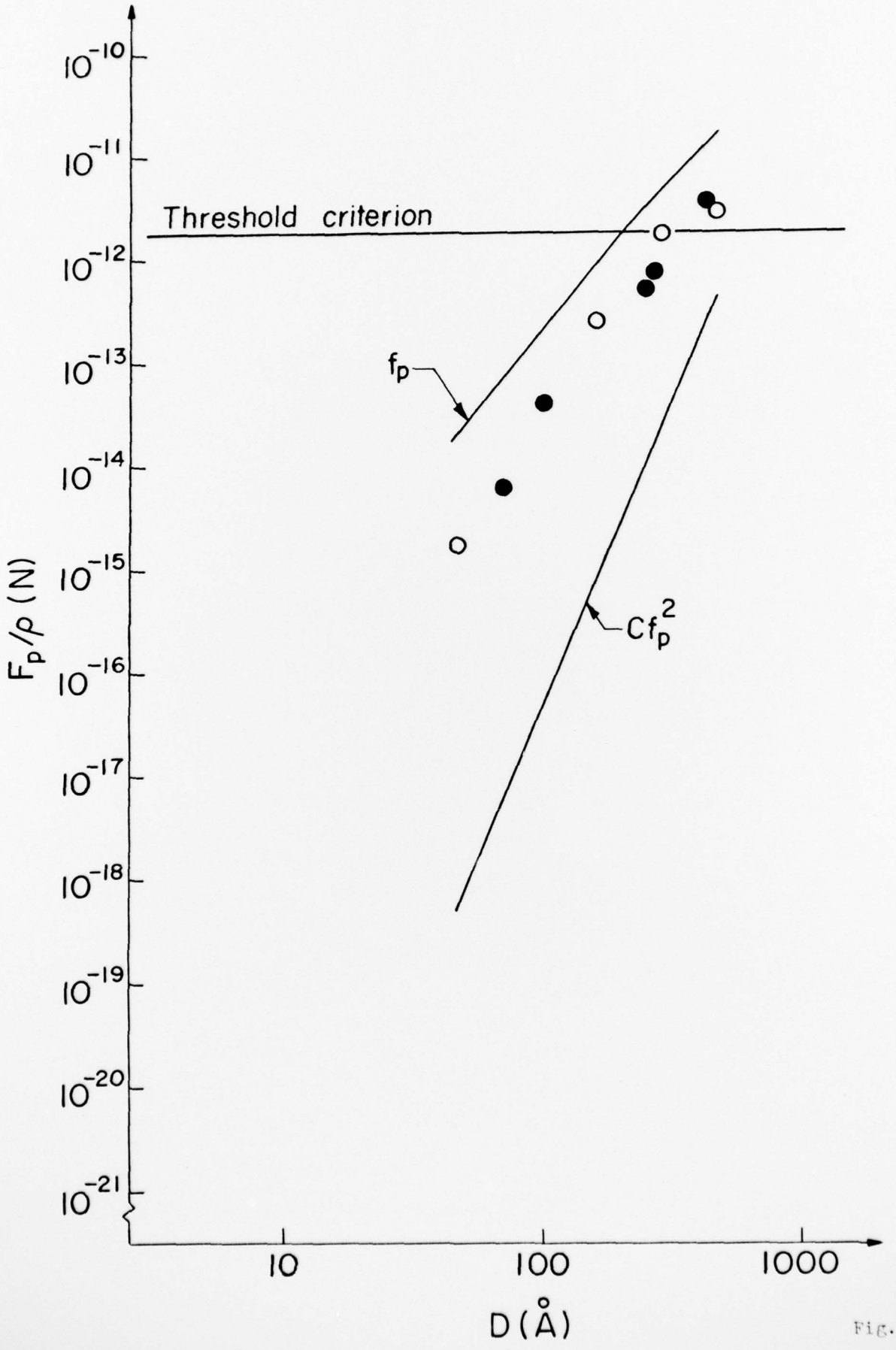
10^{-10}
10^{-11}
Threshold criterion
10^{-12}
10^{-13}
f_p
10^{-14}
10^{-15}
F_p/ρ (N)
Cf_p^2
10^{-16}
10^{-17}
10^{-18}
10^{-19}
10^{-20}
10^{-21}
10
100
1000
D (Å)

Fig. 16

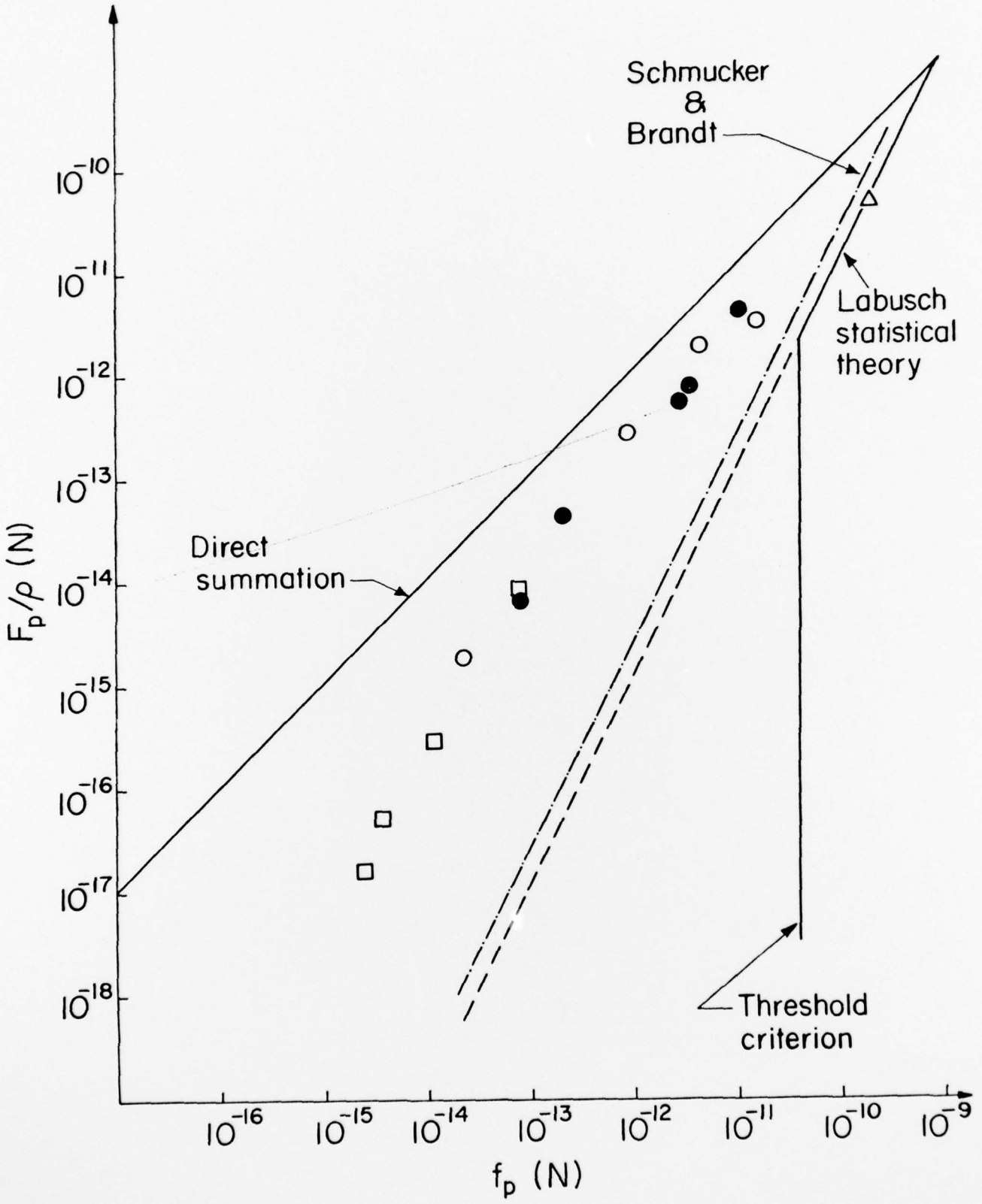
Schmucker
&
Brandt
Labusch
statistical
theory
Direct
summation
Threshold
criterion
F_p/ρ (N)
f_p (N)
10^{-10}
10^{-11}
10^{-12}
10^{-13}
10^{-14}
10^{-15}
10^{-16}
10^{-17}
10^{-18}
10^{-16}
10^{-15}
10^{-14}
10^{-13}
10^{-12}
10^{-11}
10^{-10}
10^{-9}

Fig. 17

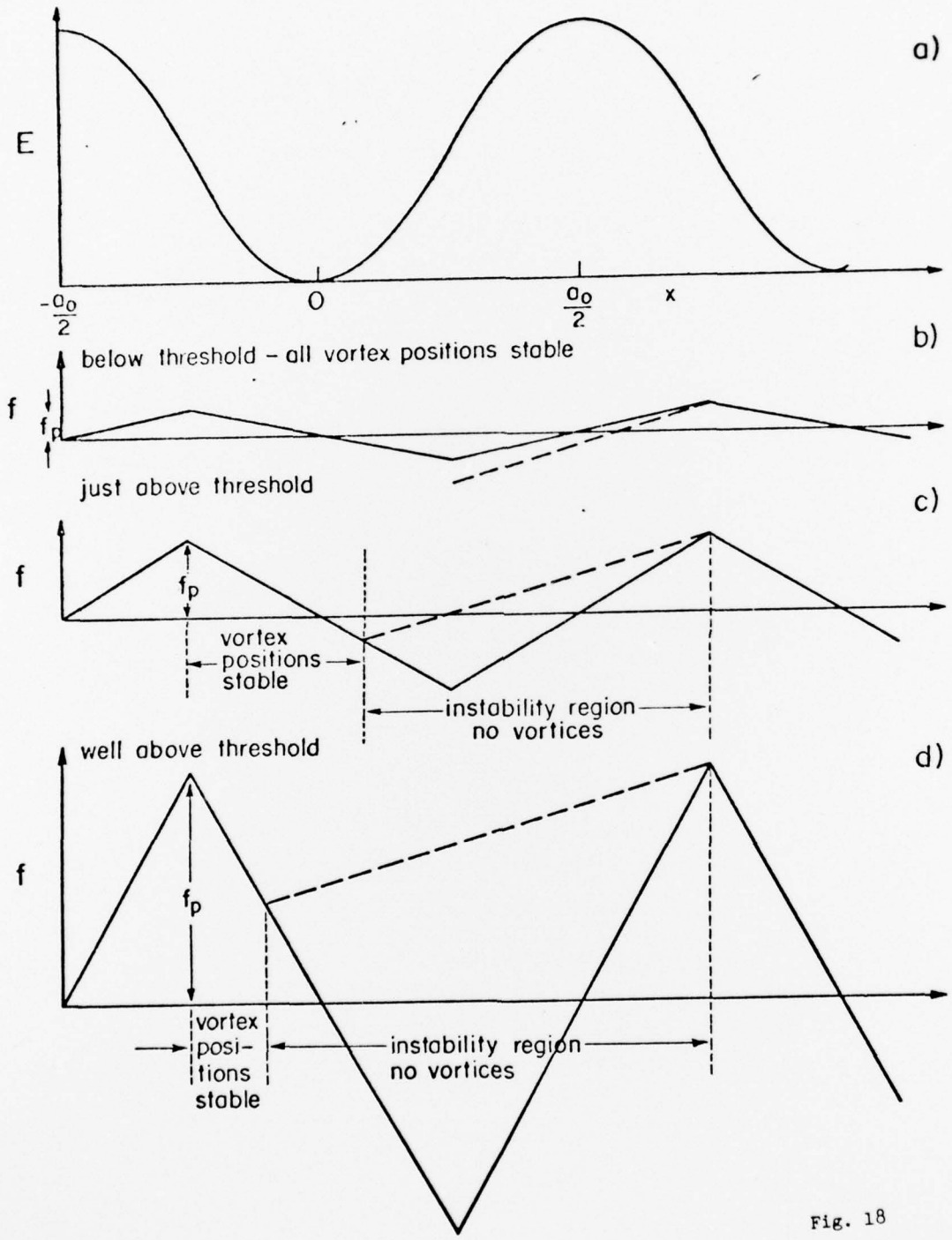
a)
E
$-\frac{a_0}{2}$
0
$\frac{a_0}{2}$
x
b)
below threshold – all vortex positions stable
f
f_p
just above threshold
c)
f
f_p
vortex positions stable
instability region no vortices
well above threshold
d)
f
f_p
vortex posi- tions stable
instability region no vortices

Fig. 18

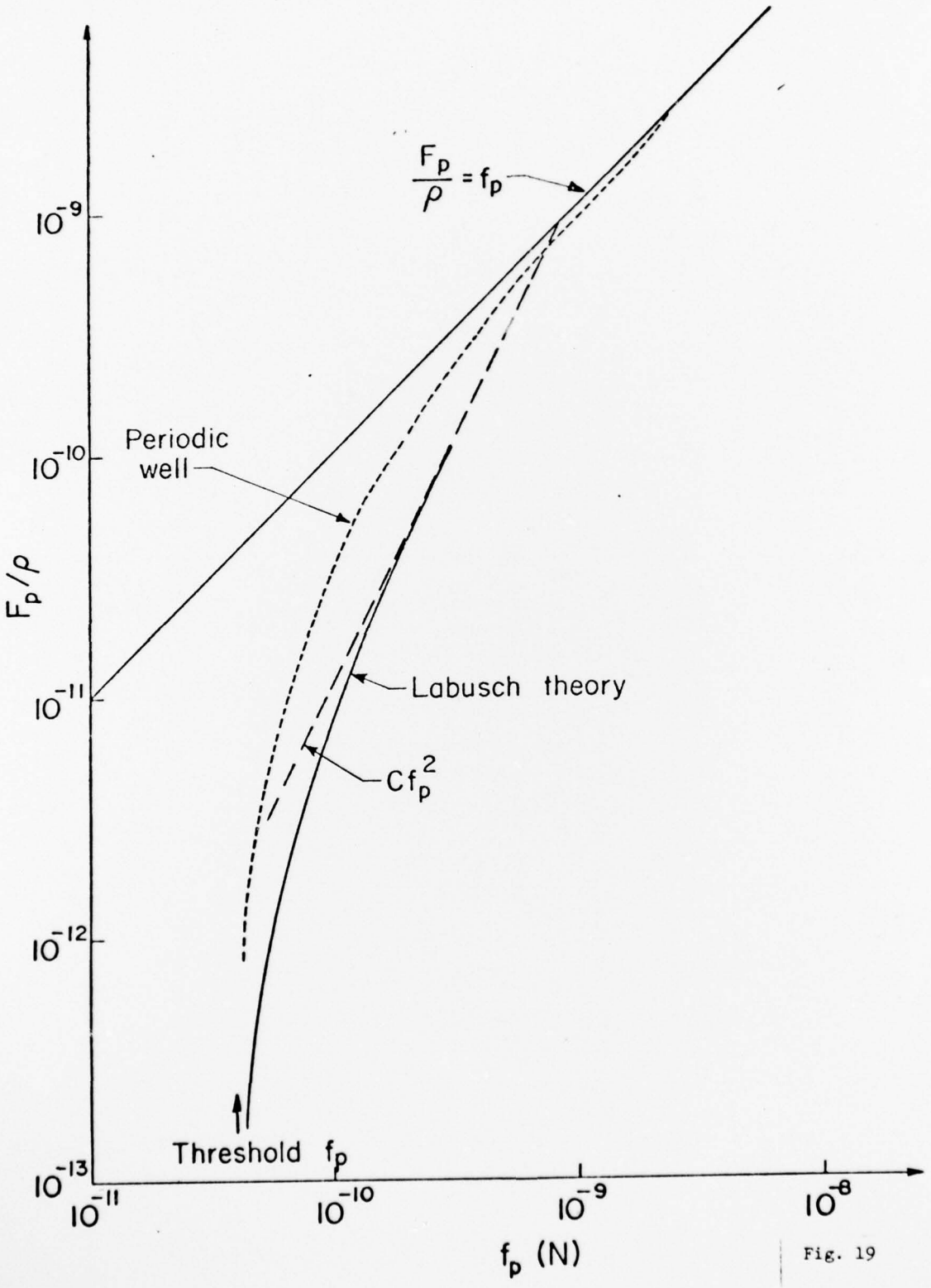
$\frac{F_p}{\rho} = f_p$
Periodic well
Labusch theory
Cf_p^2
Threshold f_p
F_p/ρ
10^{-9}
10^{-10}
10^{-11}
10^{-12}
10^{-13}
10^{-11}
10^{-10}
10^{-9}
10^{-8}
f_p (N)

Fig. 19

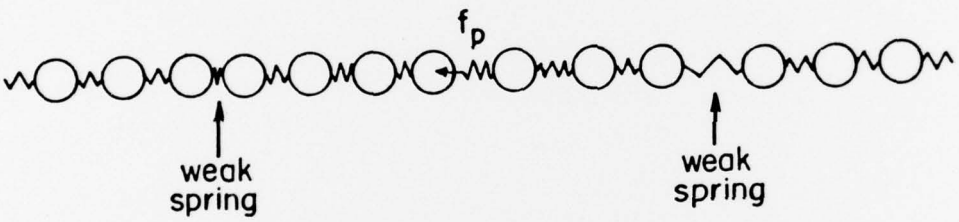

Fig. 20

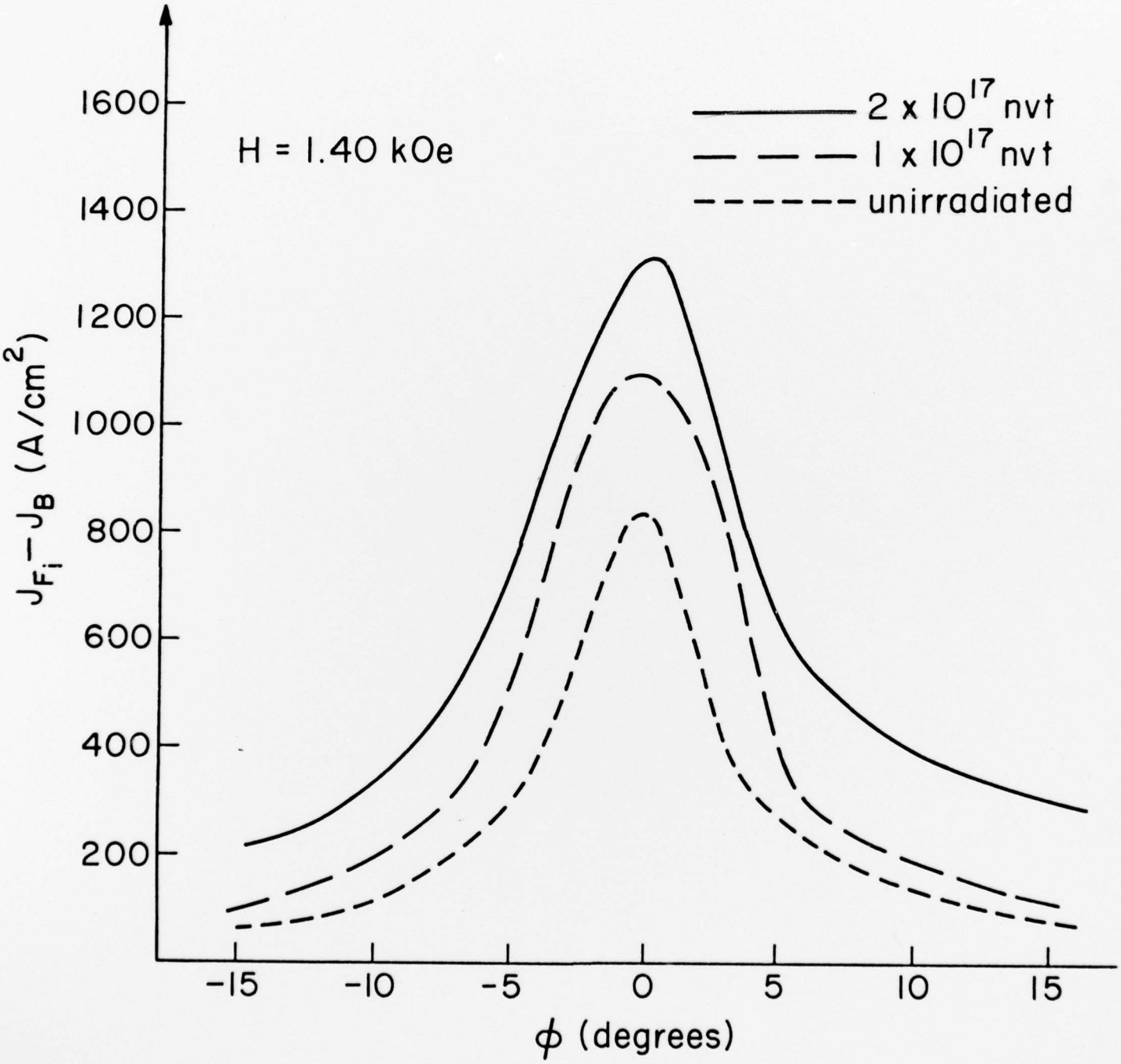
H = 1.40 kOe
2 x 10^17 nvt
1 x 10^17 nvt
unirradiated
1600
1400
1200
1000
800
600
400
200
J_Fi − J_B (A/cm^2)
-15
-10
-5
0
5
10
15
φ (degrees)

Fig. 21